Physiological and Mechanistic Dissection of *Vibrio cholerae* Stringent Response : Implications for Cholera Treatment

Hwa Young Kim

Department Medical Science

The Graduate School, Yonsei University

Physiological and Mechanistic Dissection of *Vibrio cholerae* Stringent Response : Implications for Cholera Treatment

Directed by Professor Sang Sung Yoon

The Doctoral Dissertation
submitted to the Department of Medical Science,
the Graduate School of Yonsei University
in partial fulfillment of the requirements for the
degree of Doctor of Philosophy

Hwa Young Kim

December 2020

This certifies that the Doctoral Dissertation of Hwa Young Kim is approved.

Thesis Supervisor : Sang Sun Yoon

Thesis Committee Member#1 : Dong Eun Yong

Thesis Committee Member#2 : Seok Hoon Jeong

Thesis Committee Member#3 : Yeong-Jae Seok

Thesis Committee Member#4 : Jang Won Yoon

The Graduate School
Yonsei University

December 2020

ACKNOWLEDGEMENTS

지난 6 년 간의 학위과정을 마치며 긴 시간동안 저를 한 사람의 과학자로 만들기 위해 도움을 주신 많은 분들께 진심으로 감사드립니다.

학위기간동안 제가 다양한 실험을 진행하며 여러 번 길을 잃고 헤매는 순간이 많았음에도 뒤에서 든든하게 이정표를 제시해주시고, 제 스스로 찾기 힘들었을 여러 기회도 저에게 안겨 주셨던 윤상선 교수님께 진심으로 감사드립니다.

뜻밖의 코로나 시국으로 인해 많은 일정에 차질이 있었음에도 바쁜 시간을 쪼개어 학위논문 심사위원을 맡아주신 용동은 교수님, 정석훈 교수님, 석영재 교수님, 윤장원 교수님께도 감사드립니다. 교수님들께서 관심을 가져주신 덕분에 무사히 학위과정을 마무리할 수 있었습니다.

실험실에 처음 들어왔던 2014 년 가을부터 지금까지 정말 많은 분들과 잊지 못할 추억을 쌓을 수 있어서 제가 참 인복을 많이 받았다고 생각합니다. 항상 저희 실험실에서 묵묵히 중심을 잘 잡아 주시는 이강무 박사님, 생경한 여러 실험에 대해 기본적인 이해를 도와 주시는 윤미영 박사님, 실험에 대한 기본적인 경험도

부족한 상태로 들어왔던 저를 앞에서 이끌어 주셨던 오영택 박사님, 작년부터 함께 합을 맞추어 선배로서 많은 도움을 주시는 김지은 박사님께 감사드립니다. 지금은 이 실험실을 떠났지만 선배 혹은 후배로서 많은 도움을 주었던 기훈쌤, 준혁쌤, 지연쌤, 혜진언니, 예슬이, 동근오빠, 태강쌤 그리고 소원쌤 모두 감사드립니다. 지금도 함께 실험실 생활을 하는 학생들 모두 고마웠습니다. 학위기간 내내 가장 많이 지지고 볶았던 경배쌤은 본인의 강점을 잘 살려서 하고 싶은 일을 찾아 나아가길 바랍니다. 타지에서 힘들게 공부하지만 늘 긍정적인 Mohammed 도 긴 학위기간이 지나면 꼭 꿈을 이루길 바랍니다. 처음 해보는 인포매틱스를 하느라 고생 많았던 원태오빠도 남은 학위를 잘 마치고 박사학위를 받길 바랍니다. 칙칙한 실험실 분위기를 언제나 밝게 끌어올려주는 분위기 메이커 진선언니도 아프지 말고 건강하게 학위를 잘 이어 나가길 바랍니다. 또한 저보다 늦게 들어왔지만 인생선배로서 든든하게 우리 실험실 식구들을 이끌어주는 광희쌤, 찬민쌤도 언제나 잘 해왔듯이 앞으로도 다 잘 해낼 수 있을 것이라고 생각합니다. 제가 다소 무뚝뚝한 선배임에도 항상 명랑하게 힘을 실어주는 지현이, 다현이, 채영이, 준범이도 아직

길다고 느껴질 수 있는 학위를 모두 잘 마칠 수 있으리라 생각합니다. 그리고 특유의 활달함과 똑 부러지는 모습으로 제게 많은 귀감이 된 리나쌤도 항상 잘 되기를 바랍니다. 요즘은 실험실이 떨어져 있어서 자주 보기는 힘들지만 항상 반가운 윤이쌤, 지원이도 고마웠습니다. 그리고 의대에 있을 때부터 졸업하는 이번 학기까지 함께 고생한 유진언니, 처음 써보는 장비나 실험에 어려운 일이 있을 때마다 기꺼이 도와 주신 고시환쌤께도 감사 인사를 전합니다.

무엇보다도 제가 여기까지 올 수 있도록 기나긴 마라톤을 함께 달려 주시고 저를 아낌없이 응원해주시고 지원해주신 저의 부모님께 정말 많이 사랑하고 감사하다고 말씀드리고 싶습니다. 새로운 시작을 앞둔 새내기 과학자로서 부끄럽지 않은 딸이 되기 위해 끊임없이 노력하겠습니다.

2020 년 겨울, 논문을 마무리하며 감사의 말을 전합니다.

김화영

TABLE OF CONTENTS

LIST OF FIGURES

LIST OF TABLES

ABSTRACT

Physiological and Mechanistic Dissection of *Vibrio cholerae* Stringent Response : Implications of cholera treatment

Hwa Young Kim

Department of Medical Science
The Graduate School, Yonsei University

(Directed by Professor Sang Sun Yoon)

Vibrio cholerae is the causative agent of acute diarrheal disease, cholera. To acquire pathogenic properties, *V. cholerae* expresses various virulence factors such as cholera toxin (CT), and toxin-co-regulated pilus (TCP) and these factors contribute to deadly watery diarrhea from the host intestine. When *V. cholerae* encounters growth inhibition stresses, it activates (p)ppGpp-mediated stringent response (SR). Here, we show that the bacterial capability to produce (p)ppGpp plays a critical role in antibiotic tolerance (Part II). And we further show that RelV, a novel SR enzyme in *V. cholerae*, can produce toxigenic nucleotide molecules for stringent response (Part III).

Over decades, clinical isolates of *V. cholerae* have shown resistance against many antibiotics, but the mechanistic details of the resistance are still unclear. Herein, we found that N16961, a 7th pandemic O1 *V. cholerae* strain and its isogenic Δ*relA*Δ*spoT* mutant that accumulates intracellular (p)ppGpp, were more resistant against antibiotics, compared to the Δ*relA*Δ*relV*Δ*spoT* (i.e.

(p)ppGpp^0) and Δ*dksA* mutants, which cannot produce or utilize (p)ppGpp, respectively. A genetic screening and transcriptome analysis identified that expression of many tricaboxylic acid (TCA) cycle enzyme genes was increased in the (p)ppGpp^0 strain compared to the antibiotic-resistant Δ*relA*Δ*spoT* mutant and additional deletion of those genes causes increase antibiotic tolerance of (p)ppGpp^0 strain. Together, these data suggest that (p)ppGpp suppresses the TCA cycle activity, and it may entail the antibiotic resistance. Importantly, the (p)ppGpp^0 mutant became antibiotic-tolerant, when grown anaerobically or incubated with an iron chelator. These results suggest that reactive oxygen species (ROS), whose production is affected by intracellular iron level, are involved in antibiotic-mediated bacterial killing. Consistently, ROS production was markedly increased in antibiotic-susceptible mutants upon tetracycline treatment. Iron (III) ABC transporter substrate-binding protein (FbpA) was synthesized 10-fold higher in the antibiotic-sensitive (p)ppGpp^0 mutant and the deletion of the *fbpA* gene restored the viability of the mutant. We also observed that FbpA production was repressed in the (p)ppGpp-accumulated mutant, and this entailed the reduction of intracellular free iron, the source of the Fenton reaction. Together, we demonstrated that the suppression of central metabolism and iron uptake by (p)ppGpp accumulation reduced the oxidative stress following antibiotic treatment in *V. cholerae*.

When *V. cholerae*, a causative agent of Cholera, encounters growth-

inhibitory stresses, it activates stringent response (SR) mediated by the accumulation of (p)ppGpp, a nucleotide alarmone. Three enzymes RelA, RelV and SpoT control *V. cholerae* SR, with the first two synthesizing the alarmone, while SpoT hydrolyzes it. It remains elusive, however, what specific roles RelA or RelV is playing under various conditions. When *relA* or *relV* gene was expressed in a Δ*relA*Δ*relV*Δ*spoT* triple mutant, distinct patterns of growth arrest were observed between the two conditions. The result from Two-dimensional thin layer chromatography (TLC) analysis unveiled that RelV contributes to the production of a range of different nucleotide alaromones, while RelA was not as active as was described so far in alarmone biosynthesis. RNA sequencing analysis revealed that discrete sets of genes were regulated in *relV*- and *relA*-expressing cells, respectively, with a larger number of genes being regulated by RelV. Genes involved in amino acid biosynthesis, a well-known pathway activated by bacterial SR, were highly upregulated by RelV-mediated and not by RelA-mediated activity. Furthermore, the expression of virulence-associated genes including *ctxAB* was enhanced by RelV activity. Together, our results demonstrate that RelV participates more actively in regulating *V. cholerae* SR in comparison with RelA, considered as a prototype alarmone synthetase in Gram-negatives. We are expecting the findings provided here to be useful, when establishing strategic control measures against Cholera-associated infections.

Key words : *Vibrio cholerae*, Stringent response, antibiotic tolerance, alarmone

Physiological and Mechanistic Dissection of *Vibrio cholerae* Stringent Response : Implications of cholera treatment

Hwa Young Kim

Department of Medical Science
The Graduate School, Yonsei University

(Directed by Professor Sang Sun Yoon)

Chapter I. Introduction of bacterial stringent response and *Vibrio cholerae* virulence factors

1. What is the Stringent Response?

The term "stringent" strain mostly refers to *Escherichia coli* under amino acid starvation that brings about dramatical decrease in the synthesis of DNA, stable RNA and ribosomal proteins.[1] From the stringent cell extract, Cashel and Gallant first visualized two spots by thin-layer chromatography, tentatively called as "magic spots". They were later identified to be the hyperphosphorylated guanosine derivatives ppGpp (guanosine tetra-phosphate) and pppGpp (guanosine penta-phosphate), collectively referred to as (p)ppGpp or nucleotide alarmones.[1,2] (p)ppGpp is responsible for activating a conserved stress response to nutrient starvation in bacteria. This response against multiple stress is named as stringent response (SR). Upon nutrient limitation, the bacteria rapidly accumulate (p)ppGpp, a nucleotide molecule which can

reprogram transcription globally by cooperating with RNA polymerase (RNAP) directly and regulate RNAP σ-factor indirectly.[3-5]

Intracellular (p)ppGpp concentration is controlled by RelA and SpoT classified in two different classes of enzymes.[6-9] RelA is a monofunctional synthetase that's only capable of producing pppGpp by using ATP and GTP, later converted to ppGpp. The bifunctional synthetase-hydrolase enzyme, SpoT, Rel and RSH (RelA-SpoT homologue) not only can generate (p)ppGpp but also hydrolyze the generated alarmones to either GDP and pyrophosphate (PP_i), or GTP and PP_i respectively.[6-9] Both RelA and SpoT proteins are conserved in gram-negative bacteria to control the cellular pool of (p)ppGpp through its either monofunctional or bifunctional mechanism, respectively. Regulation of these enzymes is the key for bacteria to rapidly adapt to various stress conditions by synthesizing and degrading (p)ppGpp. In case of RelA, its stimulation of enzyme activity occurs when encountering uncharged tRNAs at ribosomal A sites.[9] In contrast, SpoT proteins engage to act against a variety of nutrient stresses, such as phosphate, carbon, iron or fatty acid starvation.[6,10,11]

(p)ppGpp affects varieties of transcriptome by interacting directly with RNAP, accompanying its synergist, DnaK suppressor (DksA) protein. DksA protein binds to secondary channel of RNAP and amplifies the impact of (p)ppGpp by increasing the binding affinity.[12] (p)ppGpp and DksA can also alter transcription by regulating σ-factor competition, known as indirect regulation.[13] When the SR is evoked, (p)ppGpp inhibits RNAP binding to σ^{70}-

dependent promoters fundamental for bacterial growth in exponential phase. Consequently, the alternative σ-factors that respond to particular-stresses have ability to bind to core RNAP.[14] In addition to promoter regulation, (p)ppGpp manipulates various bacterial cell phenotypes. (p)ppGpp coordinates the ribosomal synthesis to hinder the growth rate of replicating bacterial cells, and inhibition of DNA replication occurs simultaneously resulting from accumulated alarmones.[15,16] From many recent studies, it's been revealed that this nucleotide alarmone also modulates the virulence factors of bacterial pathogen to cope with environmental and metabolic stresses.[17-20]

2. *Vibrio cholerae*

V. cholerae is a toxigenic bacterium that causes severe diarrheal disease, cholera.[21,22] Highlighted research about *V. cholerae* was conducted by Robert Koch in Egypt, 1883, though the name *V. cholerae* has been derived from Filippo Pacini, the first to discover cholera agent with curved shape phenotype, 1854.[22]

V. cholerae is usually found in aquatic environments, including brackish water and estuaries.[21,23] Over the decades, several cholera pandemics swept the world, remaining substantial number of casualties. Though cholera victims suffer from mild pain, severe dehydration derived from diarrhea can lead to death due to massive loss of body fluids. *V. cholerae* infection occurs when host drinks the contaminated water or food with toxigenic *V. cholerae*.[22,24] Since the

pathogens are transmitted through watery stool, the disease is feasible to spread from person to person rapidly. Due to the development of water supply facilities, the number of cholera patients has decreased significantly. However, in developing countries, it is still a challenge to alleviate the mortality from cholera.[25] Once entering the host, *V. cholerae* starts to dominate host intestine in acute manner, where it expresses pathogenicity by varieties of virulence factors, such as (i) cholera toxin (CT) and (ii) toxin-co-regulated pilus (TCP), the major agents of voluminous watery diarrhea.[17,21,22]

V. cholerae species is heterogeneous with regard to its pathogenic potential.[22] The criteria within the species are individualized based on each feature of cholera toxin production, serogroup and potential for epidemic spread. Serogroup is the major surface antigen characterized in *V. cholerae*, also known as O antigen.[22] In detail, when each O group is defined by identification, these antigens of *V. cholerae* can be classified from O1 to O139. Out of classified 139 serogroups, only O1 and O139 have been associated with epidemic outbreak, and none of the other 137 serogroups has led to large epidemics or extensive pandemics. The pathogenic O1 serogroup can be further subdivided into serotypes called Ogawa and Inaba.[26] Also, this serogroup can be divided into two biotypes, classical and El Tor. Classical and El Tor biotypes are major agent of 6^{th} and 7^{th} pandemic, respectively.[22] O139, another pathogenic serogroup, was first discovered lately in 1993.[27]

3. *V. cholerae* virulence factors

In *V. cholerae*, CT and TCP are responsible for major symptom of cholera.[21] The structure of CT is typical type of A-B subunit toxins of which each subunit harbors its own specific function. CT consists of homo-pentameric B subunits and a single A subunit. Pentameric B subunits serves to bind the gangliosides of intestinal epithelial cells, and the A subunit possesses a specific intracellular enzymatic function.[22] Here, TCP plays the primary role as the only colonization factor of *V. cholerae* for successful binding to host intestine.[28] In addition, infection experiments with TCP defective mutant strain reported that this pilus seems to be the key factor to cause diarrhea and significant immune response. When *V. cholerae* binds to the intestine with a help of TCP, it allows CT to bind to the gangliosides G_{M1} receptor via B subunit pentamer, the A subunit enters the epithelial cell and proteolytical cleavage catalyzes A_1 and A_2 peptides from A subunit.[29] The intracellular target of CT is adenylate cyclase of the eukaryotic cells, which mediates the transformation of ATP to cyclic AMP (cAMP).[30] The ADP-ribosylation activity of A_1 peptide enhances the intracellular cAMP concentration that leads to increased Cl^- secretion carried out by crypt cells and decreased NaCl uptake by villus cells. This ion imbalance makes massive water escaping from epithelial cells to intestinal lumen, resulting in severe diarrhea.[30]

There are cascade systems involved in the regulation of virulence genes in *V. cholerae*. ToxR, the master regulator of virulence genes, responses to environmental conditions.[22,31] ToxR protein binds to upstream tandem sequence

of *ctxAB* and increase the transcription of *ctxAB*, resulting in higher levels of CT expression. ToxR regulates not only *ctxAB* but also TCP, OMP and lipoproteins.[21,32] Except for the *ctxAB* genes, other genes in the ToxR regulon are controlled by ToxT protein.[33] Expression of CT, TCP and other virulence factors differs between the classical and El Tor biotypes.[21,34]

Many *V. cholerae* strains inhabiting in aquatic environment is known to show biofilm formation or viable but none culturable (VBNC) states.[35,36] As *V. cholerae* can transit to host intestinal tract with its biofilm cluster formation, biofilm enables the access of the bacteria into the small intestine. The *Vibrio* polysaccharide (VPS), an exo-polysaccharide, enables them to form stable biofilms and persist to various environmental stresses.[20] There are two transcriptional activators of *vps* operons, VpsR and VpsT.[37] Since VpsR is a strong activator of biofilm formation, *vpsR* gene deletion mutants are completely defective in biofilm formation. Biofilm formation is also linked to quorum sensing, a cell density dependent phenomenon.[37] Quorum sensing controls the expression of *vpsR* and *vpsT* genes through *hapR*, quorum sensing transcriptional regulator.[20] HapR down-regulates the expression of *vpsR* and *vpsT* genes by directly binding on the promoters, at high cell density.

4. Stringent response conjures *V. cholerae* virulence factors

In the host environment, pathogenic bacteria alter their metabolism in response to local conditions. To overcome unfavorable defenses of their hosts,

pathogens acquire virulence factors to make the environment favorable, such as tissue cell invasion[38] and toxic molecules secretion.[19] Ultimately, changes in nutrient supply or host immune response can trigger bacterial stringent response to adapt toward host treats. Stringent response regulates specialized secretion systems,[19] motility components,[39] or adhesins[17] to gain an advantage for nutrient acquisition. Recent studies revealed that pathogenic bacteria utilizing (p)ppGpp is critical for survival, replication and transmission.[40,41]

V. cholerae has the ability to survive and live on when it transits to human gastrointestinal tract by expressing its virulence factors on an appropriate time point.[21,22] Recent studies described that *V. cholerae* exerts pathogenic properties with the regulation of SR.[19,20,40,41] Like many other gram-negative bacteria, *V. cholerae* has RelA and SpoT as two critical enzymes for (p)ppGpp control.[17] Moreover, recently discovered small RSH homologue, RelV is also reported to contribute to (p)ppGpp synthesis in *V. cholerae*.[42] Interestingly, in case of *V. cholerae*, Δ*relA*Δ*spoT* double deletion mutant can accumulate (p)ppGpp beyond the basal level, without SpoT hydrolase activity.[19,42] And Δ*relA*Δ*relV*Δ*spoT* mutant (as known as (p)ppGpp^0), defective for (p)ppGpp producing, cannot produce CT under anaerobic TMAO respiration[19] where *V. cholerae* produce large amounts of CT. In vivo experiment with (p)ppGpp^0 mutant strain provided supplementary data to it, as down-regulation of enterotoxin resulted in significant decrease of mouse mortality. Besides, previous studies revealed that *relA* mutant defective for (p)ppGpp accumulation

during amino acid starvation displayed significantly low levels of ToxR and ToxT protein, the upstream regulator of CT and TCP.[43] At the end, SR ability of *V. cholerae* demonstrates its critical role on survival over a variety of environmental stresses via regulating bacterial motility,[39] glucose fermentation,[40] and moreover, mucosal escaping from small intestine.[44]

SR is also known to serves biofilm formation. It's been elucidated that *V. cholerae* mutants defective in SR had a reduced ability to form biofilm.[20] Defect in SR was elicited by the absence of RelA, RelV, and SpoT, decreasing the expression of biofilm formation regulator VpsR. Above all, RelV displayed the strongest effect on vpsR transcription. Consistent to this data, during anaerobic TMAO respiration, Δ*relA* mutant produced relatively higher level of CT compared with Δ*relV* mutant.[19]

These are how RelA, RelV and SpoT contribute to *V. cholerae* virulence factors in each different manner. Still, further elucidation is required to elaborate complex mechanism of the three enzymes, and how the sensing and expression occur according to the environmental stimuli. Previously, numerous research was attempted to reveal the relationship of SR and *V. cholerae* virulence. Recently, the chemical library screening was conducted with the purpose of developing a medicine that can restrain *V. cholerae* viabilities by disturbing SR ability.[45] For such purposes, unveiling SR mechanism of *V. cholerae* and understanding the cholera pathogenesis are substantially critical. In this study, we focus on discovering the aspects of SR effects on *V. cholerae*

antibiotic tolerance using phenotypic and metabolic analysis. Moreover, we describe a novel RelV product that affects bacterial viability in its intrinsic manner irrelevant to (p)ppGpp.

Chapter II. Guanosine tetra- and pentaphosphate increase antibiotic tolerance by reducing reactive oxygen species production in *Vibrio cholerae*

1. INTRODUCTION

Cholera, the epidemic acute diarrheal disease caused by *Vibrio cholerae*, occurs in many developing countries which have poor sanitation.[21] The toxigenic strains express various pathogenic factors, including toxin-co-regulated pillus (TCP) and cholera toxin (CT) to acquire the host environmental niche where it survives in the acidic gastric conditions and enters the small intestine.[21,46-49] These virulence factors permit substantial fluid transport from epithelial cells to lumen and leads to severe watery diarrhea. Thus, treatments mainly used for cholera patients are oral or intravenous hydration therapy that are effective for reducing stool output.[50] According to the cholera treatment guidelines from the WHO and the CDC (Centers for Disease Control and Prevention), antibiotic treatment in conjunction with an oral rehydration solution (ORS) is recommended for patients that have severe symptoms or are seriously dehydrated and continue to pass a large amount of stool.[24] By evaluating many antibiotics, those that are effective at (i) reducing stool output, (ii) reducing the duration of diarrhea, and (iii) induction of bacterial shedding have been selected for treating cholera patients.[51-55] Antibiotic treatment in conjunction with ORS allows patients to more rapidly recover compared to

ORS treatment alone. Tetracycline is the most effective antibiotic to reduce the cholera morbidity. However, doxycycline, a proxy for tetracycline, is currently the first-line drug of choice for cholera treatment due to its easy administration and low dosage requirement compared to tetracycline.[56] Alternative drugs for treatment include chloramphenicol, erythromycin, azithromycin, and furazolidone. This provides drug treatment flexibility dependent on infected regions or antibiotic resistance rates. These antibiotics are only administered in combination with rehydration therapy and are not permitted to using for the prophylaxis of cholera infection to prevent the induction of antibiotic resistance.[57,58] Recently, most isolates of *V. cholerae* O1 serotype from patient stools showed resistance to antibiotics that are commonly used for cholera treatment,[59-63] but with no clear underlying mechanisms.

In our previous studies, we revealed that stringent response (SR) regulates *V. cholerae* viability and virulence by providing the bacterium with increased fitness in unfavorable environments.[19,40] SR is characterized as one of the global regulatory systems in bacteria, which is activated by a variety of growth-inhibiting stresses.[7] SR induces rapid adaptation under various stress conditions via (p)ppGpp accumulation.[8] (p)ppGpp, known as a stress alarmone, forms a complex with RNA polymerase and induces profound reprogramming of global gene expression, which lead to growth arrest.[9,15,64] In most Gram-negative bacteria, (p)ppGpp production is regulated by two enzymes, RelA and SpoT.[8,17] RelA, a monofunctional synthetase, recognizes the uncharged tRNA at the A

site of a ribosome and it starts to synthesize (p)ppGpp. SpoT is the bifunctional enzyme which has both synthetase and hydrolase domains but shows mostly strong hydrolysis and weak synthetase activities. In the case of *V. cholerae*, it has an additional novel (p)ppGpp synthetase called RelV which loses its N-terminal hydrolase domain.[42,65] Because this enteric pathogen encounters the host-derived immune system during infection, human intestinal environments have the potential to influence nutrient availability to and the viability of *V. cholerae*.[21,23]

Interestingly, recent studies reported that SR-mediated transcriptional switching impacts bacterial physiology and increases antibiotic resistance.[66-68] For example, (p)ppGpp accumulation raises penicillin resistance by inhibiting peptidoglycan synthesis in both Gram-positive and negative bacteria.[69-72] This is not limited to β-lactam antibiotics and the resistance to other antimicrobials is also linked to (p)ppGpp accumulation.[73,74] It has been suggested that SR-mediated growth defects reduce antibiotic sensitivity, but this hypothesis is not fully understood. Recently, some studies suggested that decreased levels of superoxide dismutase and catalase activities in SR mutants were associated with susceptibility to multi-classes of antibiotics.[18,75] This report described the famous mechanistic model that different bactericidal antibiotics, regardless of their primary drug-target, had a common pathway that generated deleterious ROS.[76] According to this concept, ROS formation following antibiotic treatment enhanced antibiotic lethality, as well as the interaction with their

traditional targets. Importantly, this ROS stress is derived from alterations of bacterial physiology, including hyperactivation of central metabolism and cellular respiration and disruption of iron homeostasis, by disrupting specific drug targets.[76-78] It might be strange that antibiotic treatment induces the overflow of metabolism, but to support this idea, many reports have described the transcriptomic and proteomic response to the bactericidal antibiotics.[76,77] Therefore, we hypothesized the potential capacity for reducing oxidative stress is essential for bacteria to survive during antibiotic treatment.

In this study, we showed that (p)ppGpp accumulation induced antibiotic resistance in *V. cholerae* by suppressing its central metabolism. We investigated the molecular basis of the specific physiology in (p)ppGpp-null *V. cholerae* that restored their viability against antibiotics when the *acnB* gene was totally abolished. Additionally, we presented that (p)ppGpp nonproducing *V. cholerae* mutant carried higher level of intracellular free iron, the crucial source of ROS production. This report provides a novel insight into the stepwise regulation of SR that contributes to defend against oxidative stress following antibiotic treatment.

2. MATERIALS AND METHODS

A. Bacterial strains and growth conditions

All of the bacterial strains and plasmids used in this study are listed in Table 1.1. Bacterial cultures were grown in Luria-Bertani medium (LB; 1% (w/v) tryptone, 0.5% (w/v) yeast extract, and 1% (w/v) sodium chloride) at 37 °C, and antibiotics were used at the following concentrations: streptomycin (Duchefa), 200 μg/ml; ampicillin (Sigma), 50 μg/ml; and kanamycin (Duchefa) 50 μg/ml. All bacterial single colonies on LB plates were picked and inoculated in LB broth for precultures and grown overnight. Precultures were diluted 100-fold in fresh LB broth for subculture and incubated at 37 °C and 220 rpm. The incubation time was dependent on experimental procedures.

Table 1.1. Bacterial strains and plasmid used in this study

Strains or plasmids	Relevant characteristic	Source
***V. cholerae* strains**		
N16961	Wild type, O1 serogroup, biotype El Tor	Lab collection
Δ*acnB*	N16961, *acnB* deleted	This study
Δ*dksA*	N16961, *dksA* deleted	This study
Δ*icd*	N16961, *icd* deleted	This study
Δ*sucDC*	N16961, *sucDC* deleted	This study
Δ*mdh*	N16961, *mdh* deleted	This study
Δ*fbpA*	N16961, *fbpA* deleted	This study
Δ*dksA*Δ*fbpA*	N16961, *dksA* and *fbpA* deleted	This study
Δ*relA*Δ*spoT*	N16961, *relA* and *spoT* deleted	[19]
(p)ppGpp^0	N16961, *relA*, *relV* and *spoT* deleted	[19]
(p)ppGpp^0*ΔacnB*	N16961, *relA*, *relV*, *spoT* and *acnB* deleted	This study
(p)ppGpp^{0}Δ*icd*	N16961, *relA*, *relV*, *spoT* and *icd* deleted	This study
(p)ppGpp^{0}Δ*sucDC*	N16961, *relA*, *relV*, *spoT* and *sucDC* deleted	This study
(p)ppGpp^{0}Δ*mdh*	N16961, *relA*, *relV*, *spoT* and *mdh* deleted	This study
(p)ppGpp^{0}Δ*fbpA*	N16961, *relA*, *relV*, *spoT* and *fbpA* deleted	This study
N16961::pVIK112+*eKatE*		[79]
***E. coli* strains**		
SM10/λpir	Km^r *thi-1 thr leu tonA lacY supE recA*::RP4–2-Tc::Mu *pir*$^+$, for conjugal transfer	Lab collection
Plasmids		
pBAD24	Amp^r, cloning vector	Lab collection
pCVD442	*sacB* suicide vector from plasmid pUM24	Lab collection
pTnKGL3	Suicide vector bearing TnKGL3, Cm^r, Km^r	Lab collection

B. Antibiotic tolerance assay

All antibiotic tolerance assays in this study were performed as previously described with a few modifications.[18] For bacterial drug experiments, we used tetracycline (Sigma), erythromycin (Sigma), chloramphenicol (Sigma).

Exponential phase bacteria: Bacteria from precultures were diluted 100-fold in LB broth and grown shaking at 37 °C until the growth reached OD_{600} 0.5. Serine hydroxamate (Sigma) 5 mM was added to some of the cultures after 1 hr growth, and further incubated for 1 hr. Aliquots were then resuspended in serial diluted antibiotic-LB media to OD_{600} 0.05 and incubated statically for 4 hrs. The colony forming units (CFU) were measured by serial dilution of individual aliquots on LB plates for statistical testing.

Stationary phase bacteria: Overnight subcultures (16 hrs) were resuspended in serial diluted antibiotics-LB aliquots to OD_{600} 0.3 and statically incubated for 4 hrs. The survival rate of individual aliquots was also measured by viable cell counting.

C. Determination of intracellular (p)ppGpp concentration by TLC

Intracellular ppGpp concentration was measured as previously described with a few modifications.[40] To detect intracellular (p)ppGpp, bacterial cells were grown aerobically with 100 μCi/ml [^{32}P] orthophosphate (PerkinElmer Life Sciences) at each growth phase. The bacterial cell cultures were extracted with cold 10 mM Tris-HCl buffer (pH 8.0). After centrifugation to remove the cell supernatant, cell pellets were resuspended with cold 10 mM Tris-HCl

buffer and 19 M formic acid, then freeze-thawed for 3 cycles. After centrifugation to remove cell debris, cell supernatants were spotted on PEI cellulose F TLC plates (Merck). The TLC plates were developed in 1.5 M KH_2PO_4 buffer (pH 3.4) in a humidified chamber and imaged with autoradiography.

D. Construction of in-frame deletion mutants

V. cholerae mutants were created by allele replacement, as previously described.[19,80] To induce mutation, 500 bp flanking sequences located at both ends of the ORF were amplified by PCR with primers listed in Table 1.2. The primers used to amplify each flanking region were carried restriction enzyme sites that were located in multiple cloning sites of pCVD442, suicide vectors. The purified forward flanking sequences were ligated in pCVD442 vector with T4 ligase and extracted vectors were transformed to heat-shock competent cells; SM10/λpir strains. The transformed cells were selected on LB plates containing ampicillin 100 μg/ml, and cloning vectors were purified from single survival colonies, following recombination of another flanking sequence going through the same steps to transformation. The SM10/λpir strains with cloned vectors and *V. cholerae* recipient strains were mixed at a ratio of 3:1 onto LB plates and incubated for 6 hrs at 37 °C. The mixed pool was suspended in fresh LB broth, and spread on LB plates containing streptomycin 200 μg/ml or ampicillin 100 μg/ml for the first step in allelic exchange. After overnight culture, for plasmid excision from the chromosome by second cross-over, single colonies

were selected and streaked on LB plates with 8% sucrose and streptomycin 200 μg/ml without NaCl. Screening of in-frame deletion sites for each colony was proceeded by PCR to identify the desired allele with primers that containing flanking sequences and ORF.

Table 1.2. Primers used in this study

Gene name	Direction	Primer sequence (5'-3')
Cloning		
Δ*acnB* left	F	GCAAGCATGCAAACCTCGTTTACCGTTACC
Δ*acnB* left	R	CTCTGAGCTCGACTTTTTCCTCTCATTGCG
Δ*acnB* right	F	TTGCGAGCTCGCAGAGTGATTGAATCCTCT
Δ*acnB* right	R	GCGACCCGGGATTTTGAATAAAGCTTTGCC
Δ*icd* left	F	TATTGCATGCTGGCTTAAAGTGTCATAAGG
Δ*icd* left	R	GTCTAAACTAGAGAACTTTCCCTATCTGTTC T
Δ*icd* right	F	TAGGGAAAGTTCTCTAGTTTAGACACCAAA AC
Δ*icd* right	R	ATGTGCATGCATACGTTCGTCCTATTGACT
Δ*sucDC* left	F	TATTGCATGCGTGATTTGCTCGCGATTAGC
Δ*sucDC* left	R	TGGAACAACACATCTACCGCGATTACTTAC TC
Δ*sucDC* right	F	AATCGCGGTAGATGTGTTGTTCCATTTGTTT A
Δ*sucDC* right	R	ATCTGAGCTCATACCTTGAGTTTGGCGCAA
Δ*mdh* left	F	AGTTGCATGCGCGATACTTTGGATTGGTTG
Δ*mdh* left	R	ATCGATTGTCGACGTAAATCTCCTTGAGAGT A
Δ*mdh* right	F	AGGAGATTTACGTCGACAATCGATTCAAGC AT
Δ*mdh* right	R	ATTAGAGCTCTGAACCAATCACTAGCGCCG
Δ*fbpA* left	F	TGCTGCATGCTTTTAGTGTGTAAAACCACT
Δ*fbpA* left	R	CGGCGAGCTCTGTATTATAGGAATGTTCAA
Δ*fbpA* right	F	TCGCGAGCTCGTAAAATCAGGGGTATAACG
Δ*fbpA* right	R	CGCGCCCGGGATACACATAAGGATAAAGTA
Arbitrary PCR		
KGL3-Mar1, 1 round	F	GGGAATCATTTGAAGGTTGGT
Arb1, 1 round	R	GGCCACGCGTCGACTAGTACNNNNNNNNNN GATAT
Arb6, 1 round	R	GGCCACGCGTCGACTAGTACNNNNNNNNNN ACGCC
KGL3-Mar2, 2 round	F	TAGCGACGCCATCTATGTGTC
Arb2, 2 round	R	GGCCACGCGTCGACTAGTAC

E. Construction of a random Tn-insertion mutant library

A Tn-inserted mutants library was constructed by using the mariner based Tn, TnKGL3, which contains a kanamycin resistance marker. Tn mutagenesis of Δ*relA*Δ*relV*Δ*spoT* (i.e. (p)ppGpp^0) mutant was performed with SM10/λpir, which carries the TnKGL3. SM10/λpir strains and the *V. cholerae* recipient strain were mixed at a ratio of 2:1 onto LB plates and incubated for 6 hrs at 37 °C. The mixed pool was suspended with fresh LB broth, and spread on LB plates containing streptomycin 200 μg/ml, kanamycin 100 μg/ml, and incubated overnight. The survival bacterial pool was harvested in LB broth, and diluted in LB aliquots containing tetracycline 50 μg/ml to OD_{600} 0.3 and statically incubated for 4 hrs. The whole bacterial cells of each aliquot were recruited for centrifugation and resuspended again in LB aliquots containing tetracycline 50 μg/ml and incubated for 4 hrs. These procedures were repeated 3 times and final aliquots were partially spread on LB plates containing streptomycin and kanamycin. The surviving bacterial colonies were collected into a library, and the Tn-insertion site for each mutant was determined by arbitrary PCR. The first round of arbitrary PCR was performed by transposon TnKGL3 specific primer, Mar1, and two random primers, Arb1 and Arb6. The following second round of PCR proceeded with Mar2 and Arb2, by using the first round PCR products for templates. The PCR products were sequenced using the primer Mar2. The Tn inserted locations were identified by comparison with the public database of the *Vibrio cholerae* genome sequence.

F. Scanning electron microscopy analysis

Characterization of bacterial cell morphology and size were visualized with scanning electron microscopy, following procedures previously described.[81] Briefly, for the sample preparation, bacterial cell cultures were fixed with PBS containing 2% glutaraldehyde and 0.1% paraformaldehyde for 2 hrs and stained with 1% OsO_4. Samples were then coated with gold by an ion sputter (IB-3 Eiko, Japan) and examined with a scanning electron microscope (FE SEM S-800, Hitachi, Japan) at an acceleration voltage of 20 kV. Images were processed with ESCAN 4000 software (Bummi Universe Co., LTD, Seoul, Korea). For measuring the cell length and diameter, more than 100 straight-lined cells were randomly chosen from the digitized SEM images and the distance between the two ends was automatically calculated.

G. RNA-sequencing analysis

Bacterial cultures grown in LB were harvested at 16 hr post inoculation. Aliquots of each cultures (n=3) were pooled together in one tubes for RNA analysis. To extract high quality bacterial RNA, an RNeasy Protect kit (Qiagen) was used with an RNeasy mini kit (Qiagen) following the manufacturer's protocol. The quantity and quality of total RNA were evaluated using RNA electropherograms (Agilent 2100 Bioanalyzer; Agilent Technologies, Waldbroon, Germany) and by assessing the RNA integrity number. From each sample with an RNA integrity number value greater than 8.0, 8 μg of the total RNA was used as a starting material and treated with the MICROBExpress™

mRNA enrichment kit (Invitrogen). The resulting mRNA samples were processed for the sequencing libraries using Illumina mRNA-Seq sample preparation kit (Illumina, San Diego, CA) following the manufacturer's protocols. One lane per sample was used for sequencing with the Illumina Genome Analyzer IIx (Illumina) to generate nondirectional, single-ended, 36-base pair reads. Quality-filtered reads were mapped to the reference genome sequences (NCBI Bio-Project accession number PRJNA57623, identification number 57623) using CLRNASeq version 0.80 (Chunlab, Seoul, Korea). Relative transcript abundance was computed by counting the RPKM.[82]

H. ROS measurement

Chemical hydrolysis of DCF-DA (2',7'-dichlorofluorescin diacetate) was performed following procedures described elsewhere.[83] Briefly, 0.5 ml of 5 mM DCF-DA, dissolved in 100 % ethanol, was reacted with 2 ml of 0.1 N NaOH at room temperature for 30 min. The reaction was stopped by adding 7.5 ml of 100 mM PBS, giving a final DCF concentration of 50 μM. Bacterial suspensions prepared from stationary phase cultures were treated with 50 μg/ml tetracycline for 1 hr. After treatment, the suspensions were centrifuged at 13,000 rpm for 3 mins and cell free supernatants were removed. Cell pellets were resuspended with 50 μM DCF solution and incubated for 30 mins. Then, the DCF intensity, which is indicative of the intracellular ROS level, was measured with a Victor X4 plate reader (Perkinelmer).

I. SDS-PAGE and protein identification

Preparation of periplasmic fractions was followed procedures previously described.[84] *V. cholerae* strains were grown anaerobically in LB for 16 hrs. Cell pellets were resuspended with PBS containing 250 μg/ml polymyxin B and incubated for 15 mins at 4 °C. After incubation, the mixtures were centrifuged at 13,000 rpm for 20 mins at 4 °C and the supernatant was used for separation of periplasmic proteins. Protein was quantified by the method of Bradford and 5 μg of proteins were separated by 12% SDS-PAGE. The SDS-PAGE gel fractions were submitted to Yonsei Proteome Research Center for protein identification.

J. Electron Paramagnetic Resonance analysis

Intracellular free iron levels were measured as described previously with a few modifications.[85] Bacterial cells were grown in LB media and harvested at 16 hrs post-inoculation. A bacterial cell pellet was resuspended in 5 ml pre-warmed fresh LB broth that contained 10 mM DETAPAC (diethylene-triaminepentaacetic acid, pH 7.0) and 20 mM desferrioxamine (pH 8.0). DETAPAC blocks further iron import, while desferrioxamine diffuses into cells and binds unincorporated iron in an EPR-visible ferric form. The concentrated cells were incubated at 37 °C for 15 mins in a shaking incubator. The cells were washed with ice cold 20 mM Tris-Cl (pH 7.4) twice. Cells were then resuspended in 200 μl of ice cold 10% glycerol/20 mM Tris-Cl (pH 7.4). The cell suspension (200 μl) then was transferred into an EPR tube and frozen in

liquid nitrogen. Ferric sulphate standards were mixed with desferrioxamine and prepared in the same Tris buffer containing glycerol. The spectrometer settings were as follows: microwave power, 1 mW; microwave frequency, 9.64 GHz; modulation amplitude, 10 Gauss at 100 KHz; temperature, 15 K.

K. Statistical analysis

The data are expressed as the means ± S.D. Unpaired Student's t tests (two-tailed, unequal variance) were used to analyze the differences between experimental groups. p values < 0.05 were considered statistically significant. All experiments were repeated for reproducibility.

3. RESULTS

A. (p)ppGpp-accumulated *V. cholerae* exhibits antibiotic tolerance

Stringent response (SR) regulates bacterial responses to overcome unfavorable growth conditions in *V. cholerae*. To explore whether *V. cholerae* develops antibiotic tolerance in an SR-dependent manner, we measured survival rates of a range of SR-related mutant strains of *V. cholerae*. Front-line drugs for cholera treatment, tetracycline (Tc), erythromycin (Em), and chloramphenicol (Cp) were used for the bacterial treatments. To elucidate whether antibiotic tolerance was specifically induced by (p)ppGpp accumulation, we first chemically induced (p)ppGpp overproduction in N16961, a 7th pandemic O1 *V. cholerae* strain. When N16961 was treated with serine hydroxamate (SHX) for 2 hrs, a serine analogue that activates SR by mimicking amino acid starvation,[18] a marked increase in (p)ppGpp production was induced (Fig. 1.1). Although ppGpp and pppGpp were not clearly distinguished in our thin layer chromatography (TLC) assay, SHX-treated N16961 produced dramatically abundant (p)ppGpp compared with untreated controls (Fig. 1.1). To assess the effect of (p)ppGpp accumulation on bacterial survival under antibiotic stress, we treated N16961 grown in LB or LB+SHX with varying concentrations of Tc, Em, or Cp for 4 hrs. Loss of viability was detected in LB-grown N16961. Complete killing was observed after 4 hrs treatment with 10 μg/ml Tc (Fig. 1.2A), 60 μg/ml Em (Fig. 1.2B) and 25 μg/ml Cp (Fig. 1.2C). SHX-treated bacterial cells, however, were tolerant to the same

antibiotic treatment and maintained their viability under conditions lethal to the control groups (Fig. 1.2A-C). Although the extent to which these changes occurred were similar in all instances, bacterial viability was least affected in the Tc-treated group, with ~10^6 CFU/ml recovered even after treatment with the 20 μg/ml concentration (Fig. 1.2A). These results suggest that a clear mechanistic link likely exists between SR and antibiotic tolerance in *V. cholerae*.

To further elucidate the effect of intracellular (p)ppGpp accumulation on bacterial susceptibility to antibiotics in *V. cholerae*, we tested isogenic Δ*relA*Δ*spoT* double and Δ*relA*Δ*relV*Δ*spoT* (termed (p)ppGpp^0) triple mutant strains. The Δ*relA*Δ*spoT* mutant showed highly elevated levels of (p)ppGpp production due to (i) the action of RelV, an additional enzyme involved in (p)ppGpp biosynthesis and (ii) the lack of SpoT that hydrolyzes (p)ppGpp.[19] The (p)ppGpp^0 mutant, which lacked all enzymes involved in (p)ppGpp metabolism, was found to produce no (p)ppGpp.[19] The level of (p)ppGpp produced in the Δ*relA*Δ*spoT* mutant was similar to that in the SHX-treated N16961 cells, while no (p)ppGpp was produced in the (p)ppGpp^0 triple mutant (Fig. 1.1). We also included a Δ*dksA* mutant, defective in DksA that binds to RNA polymerase to facilitate the function of (p)ppGpp during SR.[86] The capability of the Δ*dksA* mutant to produce (p)ppGpp was not affected as shown in Fig. 1.1. Because (p)ppGpp levels are known to accumulate as bacterial cells enter the stationary phase,[87] we also examined how each bacterial strain, harvested at either the exponential or stationary phase, responded to antibiotic

stresses.

When exponential-phase cells were treated with antibiotics, (p)ppGpp^0 and Δ*dksA* mutant strains as well as the WT strain N16961 invariably lost their viability. The Δ*relA*Δ*spoT* mutant, which accumulates intracellular (p)ppGpp, was found to be the only strain that maintained viability (Fig. 1.2D-F). In contrast, bacterial strains harvested at the stationary phase displayed marked differences from those grown in the exponential phase. While the Δ*relA*Δ*spoT* mutant continued to be antibiotic-tolerant, WT N16961 was also found to be tolerant to the same antibiotic treatment (Fig. 1.2G-I). Furthermore, these two strains developed tolerance to significantly higher concentrations of antibiotics. Their viabilities were not affected even in the presence of 50 μg/ml Tc, 600 μg/ml Em or 500 μg/ml Cp, respectively.

To further verify the role of (p)ppGpp in conferring antibiotic tolerance in *V. cholerae*, we tested the antibiotic-susceptible (p)ppGpp^0 mutant harboring pRelV$_{BAD}$, a plasmid that can express the *relV* gene via an arabinose-inducible promoter. When the *relV* gene was expressed, the mutant cells became tolerant to Tc treatment. Restored tolerance was observed in cells harvested at either growth phase. Such a restoration was not detected in the mutant transformed with a control plasmid. Together, these results demonstrated that the ability to produce and utilize (p)ppGpp, a SR regulator, was critically important in affecting *V. cholerae* susceptibility to antibiotics.

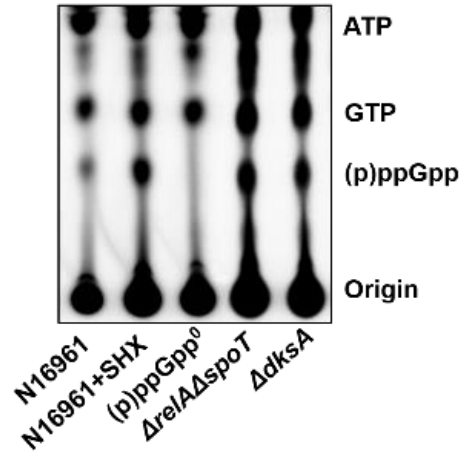

Figure 1.1. Detection of (p)ppGpp accumulation pattern in wild type N16961 by thin layer chromatography (TLC). Wild type N16961 divided into two groups and grown in LB supplemented with or without serine hydroxamate (SHX) in the presence of [^{32}P] orthophosphate for 2 hrs. Cellular extracts were prepared and analyzed in TLC. Δ*relA*Δ*spoT*, (p)ppGpp^{0} and Δ*dksA* mutants were also grown with [^{32}P] orthophosphate and processed for the TLC assay.

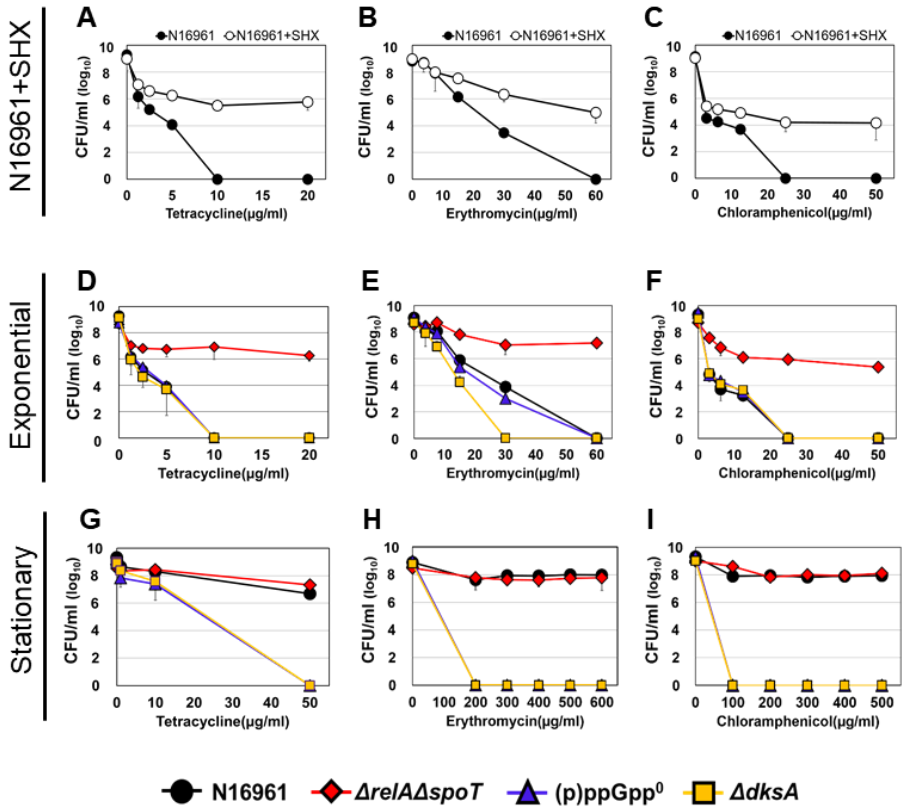

Figure 1.2. Effects of (p)ppGpp on viability of *V. cholerae* strains against clinically used antibiotics. (A-I) Bacterial viabilities under various clinically used antibiotics were measured in each growth condition. Wild type N16961 and various (p)ppGpp-associated mutant strains were inoculated in LB and aerobically grown to each growth stage. Aliquots of each culture were resuspended in several concentrations of antibiotic containing LB broth and sampled at 4 hrs post-inoculation and were 10-fold serially diluted to assess the number of CFU.

B. Mutations in the *acnB* gene resulted in increased tolerance to antibiotic stresses

To provide a mechanistic insight into the increased antibiotic susceptibility of the (p)ppGpp^0 mutant, we sought to identify additional mutations that rendered the mutant tolerant to antibiotic treatments. To achieve this goal, we constructed a Tn insertion library of the (p)ppGpp^0 mutant and looked for mutants that survived Tc treatment. Experimental procedures are described in Fig. 1.3A. After 3 successive sub-cultures in Tc-containing media, we recovered 7 mutants that exhibited unencumbered growth. Subsequent analysis indicated that these mutants harbored Tn insertions in the *acnB* gene encoding a TCA cycle enzyme, aconitase B (Fig. 1.3B). Importantly, Tn insertion was found to occur at different locations of the gene in each of these mutants (Fig. 1.3B), suggesting that independent mutational events resulted in an identical consequence. We then introduced an in-frame deletion of the *acnB* gene into N16961 and (p)ppGpp^0 mutants and measured bacterial responses to the antibiotic treatments. Notably, the viability of bacterial cells, when harvested at the exponential phase, was dramatically increased in both Δ*acnB* and the quadruple (p)ppGpp^{0}Δ*acnB* mutants compared with their parental strains (Fig. 1.4A-C). The CFUs of up to ~10^6 per ml were observed following Tc (Fig. 1.4A) and Cp (Fig. 1.4B) treatments, while ~10^4 per mL was recovered after treatment with Em (Fig. 1.4C). Bacterial cells remained viable even in the presence of the highest concentrations of antibiotics. When the (p)ppGpp^{0}Δ*acnB* quadruple

mutant, harvested at the stationary phase, was treated with antibiotics, higher levels of bacterial survival were detected (Fig. 1.4D-F).

Importantly, when the plasmid-born *acnB* gene was expressed by the arabinose-inducible promoter, bacterial strains became susceptible to Tc treatments. Consistent with previous results, sharper decreases in bacterial viability were detected when using exponential phase cells. Together, these results demonstrated that deletion of the *acnB* gene conferred a survival advantage to *V. cholerae* in the presence of antibiotic stresses.

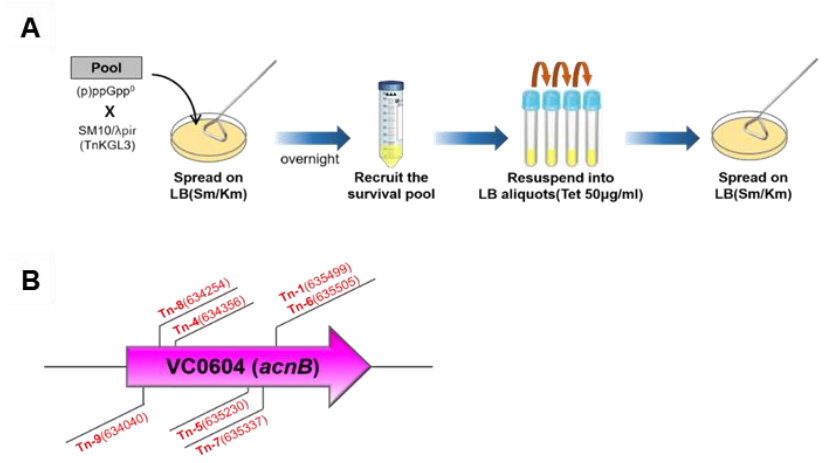

Figure 1.3. Screening of Tn insertion mutant strains, derived from the (p)ppGpp^0 strain, which recovered viability under antibiotic treatment. (A) Tn-insertion mutants, derived from the (p)ppGpp^0 mutant, that survived in the presence of a lethal concentration of tetracycline (50 μg/ml) were selected. Tetracycline was treated 3 times every 4 hrs to the entire recruited culture. (B) A genetic map of the *acnB* gene (VC0604) in *V. cholerae*. Arrowheads indicate the positions of Tn-insertions.

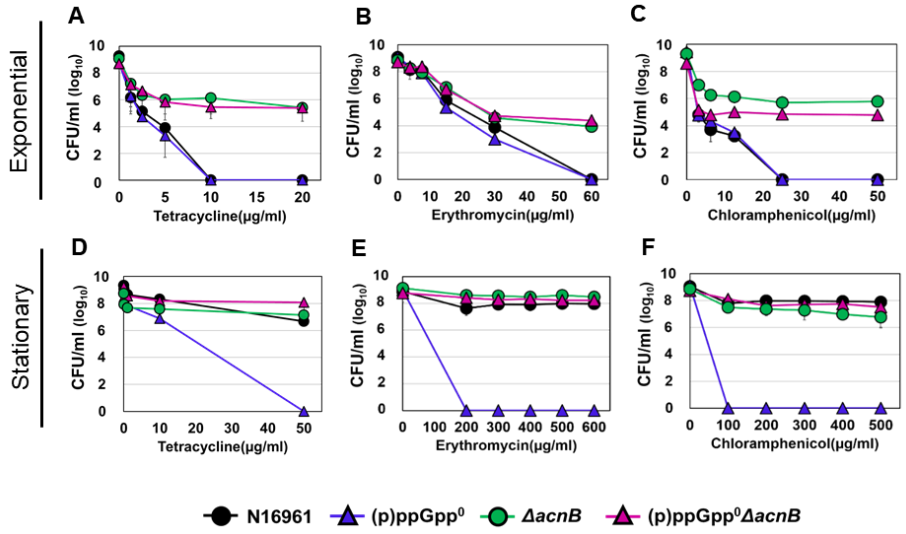

Figure 1.4. Bacterial viability of *acnB*-deletion mutants under clinically used antibiotics. (A-F) Bacterial viability of *acnB*-deletion mutants under (A, D) tetracycline, (B, E) erythromycin and (C, F) chloramphenicol treatments. Aliquots of each culture were resuspended in several concentrations of antibiotic containing LB broth and sampled at 4 hrs post-inoculation and serially diluted for CFU counting.

C. Intracellular (p)ppGpp levels inversely regulate TCA cycle activity, which affects bacterial growth and cell morphology

Aconitase B, encoded by *acnB*, is the enzyme that catalyzes the interconversion of citrate and isocitrate in the TCA cycle. To examine whether the bacterial TCA cycle was regulated depending on the intracellular concentration of (p)ppGpp, we monitored transcript levels of genes encoding TCA cycle enzymes by RNASeq analysis. First, *acnB* gene expression was ~3-fold higher in the (p)ppGpp^0 mutant than in the N16961 or in the (p)ppGpp-accumulating Δ*relA*Δ*spoT* mutant (Fig. 1.5). It is of note that N16961 also possesses the *acnA* gene that encodes a phylogenetically distinct aconitase. However, its expression was not detected in all 3 strains, indicating that aconitase B is likely the major enzyme in the TCA cycle (Fig. 1.5). Expressions of *mdh*, *gltA*, *icd*, *sucA*, *sucC* and *sucD* genes were also noticeably increased in the (p)ppGpp^0 mutant, while their expressions were decreased (albeit to varying degrees) in the Δ*relA*Δ*spoT* mutant (Fig. 1.5). Although clear (p)ppGpp-dependencies were not observed in transcriptional regulation of the *sdhA*, *sdhC*, *sdhD*, *frdB* and *ttdA* genes (Fig. 1.5), our RNASeq results strongly suggest that TCA cycle activity is inversely regulated by intracellular (p)ppGpp concentrations.

We then asked whether the (p)ppGpp-dependent regulation of TCA cycle gene expression was reflected in bacterial growth. When wild type N16961 was grown aerobically in LB media, OD_{600} values were reached at ~1.38 at 4 hr

post-inoculation and gradually increased up to ~3.5 for the rest of the experimental period (Fig. 1.6A). Consistent with a previous finding,[19] bacterial growth was significantly retarded in the Δ*relA*Δ*spoT* mutant that accumulates (p)ppGpp. Final OD_{600} values were ~2.0. In contrast, the (p)ppGpp^0 mutant exhibited faster growth compared with N16961 and final OD_{600} was reached at ~4.5 (Fig. 1.6A). Similarly, the Δ*dksA* mutant grew more vigorously, compared with N16961, further confirming that the Δ*dksA* mutant shared growth-associated phenotypes with the (p)ppGpp^0 mutant (Fig. 1.6A). To reveal the effect of *acnB* gene deletion on bacterial growth, we also monitored the growth of Δ*acnB* and (p)ppGpp^{0}Δ*acnB* mutants. Both mutants exhibited a significantly retarded growth during the early growth stage. For the first 3 hrs, their growth was comparable to that of the Δ*relA*Δ*spoT* mutant (Fig. 1.6A). Importantly, the robust growth phenotype of the (p)ppGpp^0 mutant disappeared when the *acnB* gene was additionally disrupted, further suggesting that de-repressed aerobic growth of the (p)ppGpp^0 mutant was associated with increased activity of the *acnB* gene product (Fig. 1.6A).

Elevated antibiotic resistance is observed when bacterial cells exhibit a persister phenotype that is often accompanied by cell shape changes.[35,88,89] To address this possibility, we analyzed digitized images of various bacterial strains that showed distinct antibiotic susceptibility. N16961 cells, harvested at the stationary phase that were thus more resistant to antibiotics, were shorter and thinner than those harvested at the exponential phase (Fig. 1.6B).

Antibiotic-tolerant Δ*relA*Δ*spoT* mutant and SHX-treated N16961 cells looked thinner and shorter, regardless of when they were harvested (Fig. 1.6B). In contrast, antibiotic-susceptible (p)ppGpp^0 and Δ*dksA* mutants maintained their regular curve-shaped morphotype even at the stationary phase (Fig. 1.6B). These results clearly suggest that bacterial cells with reduced size are likely more resistant to antibiotic treatment. Of particular interest is that disruption of the *acnB* gene also resulted in shorter and thinner morphotypes, a phenotype observed under (p)ppGpp-accumulating conditions (Fig. 1.6B). Together, these results demonstrated that (i) cell shape changes could be induced upon intracellular (p)ppGpp accumulation or metabolic alterations by *acnB* gene mutation and (ii) such changes are closely related to bacterial responses to antibiotic treatment.

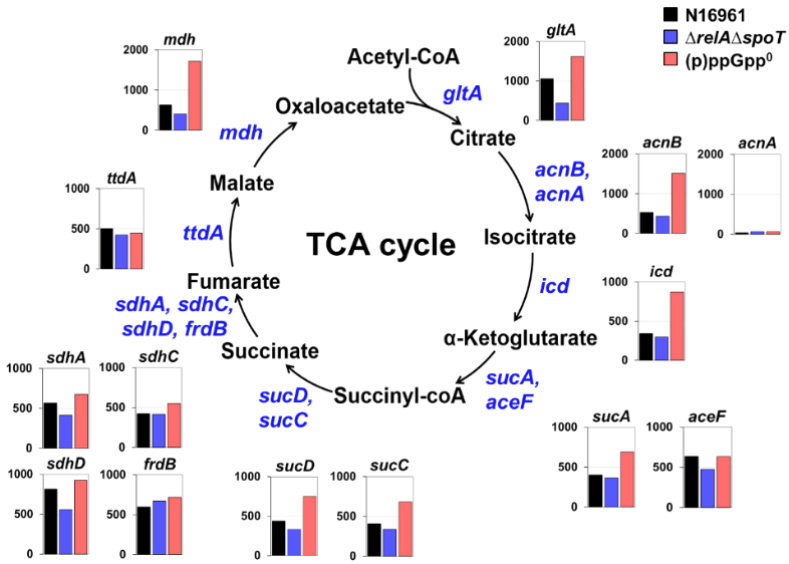

Figure 1.5. RNA-sequencing analysis of TCA cycle enzymes dependent on (p)ppGpp accumulation. RNA samples extracted from three independent bacterial cultures were pooled together for the analysis. Transcripts were extracted at 16 hrs from bacterial cells grown under LB. Each bar represents the RPKM value of the transcript.

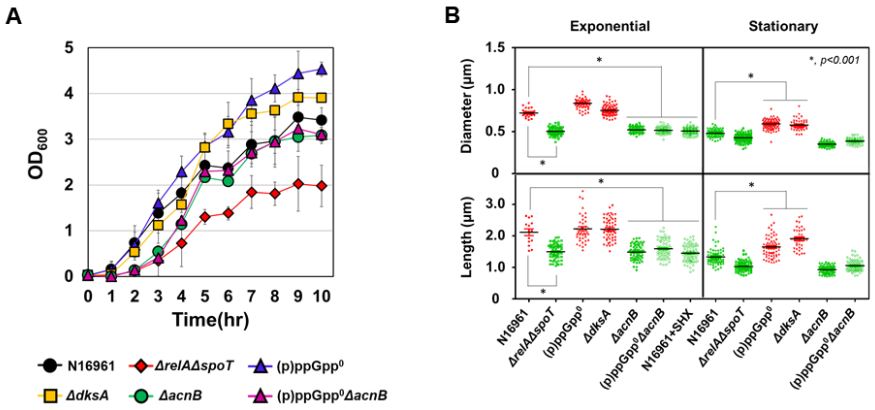

Figure 1.6. Effects of central metabolism repression on bacterial growth and cell morphology. (A) Bacterial cells were inoculated in LB and grown in aerobic conditions for 10 hrs. OD_{600} values were measured every 1 hr. (B) Scanning electron microscope (SEM) analysis of N16961 and various (p)ppGpp-associated mutant strains grown under identical conditions as seen in Fig 1. The plots show the distribution of diameter and length of each strain. The solid horizontal lines represent the geometric mean values. (*, p<0.001)

D. Other TCA cycle mutants also exhibit increased antibiotic tolerance

To see if other TCA cycle mutants also exhibit similar phenotypes to the *acnB* mutant, we additionally constructed in-frame deletion mutants of TCA cycle enzymes (Δ*icd*, Δ*sucDC* and Δ*mdh*) in both wild type N16961 and (p)ppGpp^0 mutant background and monitored their responses to the Tc treatment. As shown in Fig. 1.7, TCA cycle mutants were also found resistant to Tc. The Δ*icd* mutant showed the most similar resistance to the Δ*acnB* mutant, whereas the remaining two mutants (Δ*sucDC* and Δ*mdh*) showed lower resistance (Fig. 1.7A and C). Importantly, when each of these mutations was introduced in the antibiotic-sensitive (p)ppGpp^0 mutant, antibiotic resistance was restored (Fig. 1.7B and D). Compared to the (p)ppGpp^0 mutant, (p)ppGpp^{0}Δ*acnB* and (p)ppGpp^{0}Δ*icd* mutants maintained their viabilities at ~10^8 cells/ml following 4 hrs Tc treatment at 50 μg/ml. The (p)ppGpp^{0}Δ*sucDC* and (p)ppGpp^{0}Δ*mdh* survived ~10^6 cells/ml. Taken together, these results suggest that disruptions of the TCA cycle function either due to the mutation of *acnB* gene or other constituting genes affected antibiotic resistance in *V. cholerae*. Our results also show that ablation of *acnB* or *icd* gene, whose products mediate early steps of the TCA cycle, produced a more profound effect on bacterial responses to antibiotic stresses.

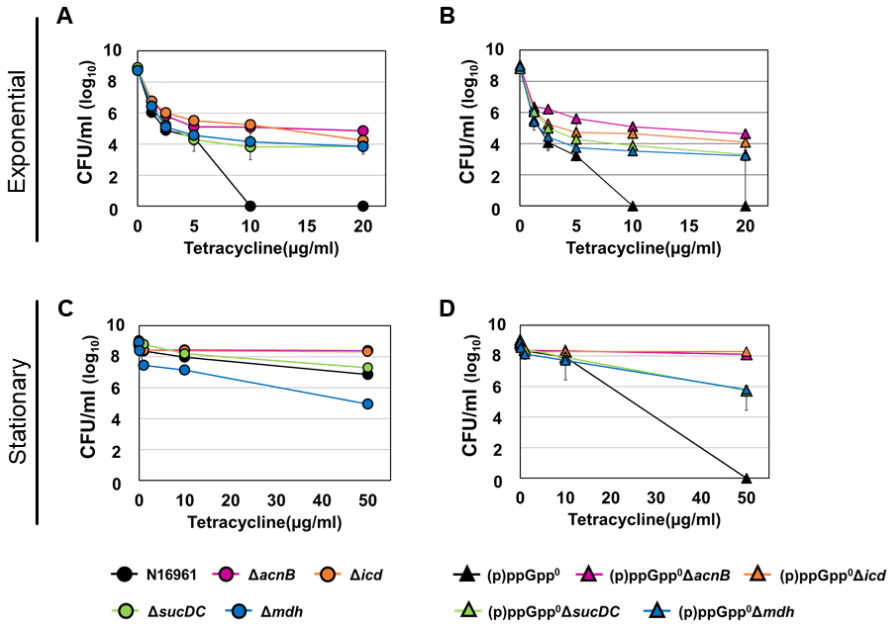

Figure 1.7. Effects of TCA cycle gene mutations on *V. cholerae* antibiotic tolerance. Bacterial viabilities under various Tc concentrations were measured. Each mutation indicated below in different colors was introduced in N16961 (A, C) and the (p)ppGpp^0 mutant (B, D). Bacterial strains were inoculated in LB and aerobically grown to exponential (A, B) or stationary phase (C, D). Experimental conditions were identical to those described in Fig. 1E and H.

E. Antibiotic-mediated bacterial killing occurs only in the presence of molecular oxygen and iron

Our results so far showed that (i) expression of TCA cycle genes such as *acnB*, *icd* and *mdh* was highly induced in the antibiotic-susceptible (p)ppGpp^0 mutant, (ii) antibiotic-mediated bacterial killing was reduced in each of these TCA cycle mutants and (iii) when (p)ppGpp was accumulated, bacterial cells shrank and became antibiotic-tolerant. These findings led us to hypothesize that (p)ppGpp accumulation results in metabolic slowdown rendering bacterial cells unresponsive to antibiotics. To explore whether active metabolism, possibly fueled by aerobic respiration, is necessary for antibiotic-mediated bacterial killing, we compared bacterial responses under aerobic vs. anaerobic environments. Exponential phase N16961 cells, which were found to be antibiotic-sensitive, maintained their viability when further grown for 4 hrs anaerobically with Tc (Fig. 1.8A). Anaerobiosis also provided an additional protective effect (>10-fold) on stationary phase N16961 cells against 50 μg/ml Tc (Fig. 1.8D). Likewise, only marginal viability loss was observed upon treatment with Tc in two antibiotic-sensitive mutants, (p)ppGpp^0 (Fig. 1.8B and E) and Δ*dksA* (Fig. 1.8C and F), under strict anaerobic environments. These results demonstrated that antibiotic-mediated bacterial killing occurred only during aerobic growth.

Hydroxyl radical (OH·), the most bactericidal ROS, was reported to be produced during antibiotic treatments in large quantities.[76] Because its

production is catalyzed by the iron-mediated Fenton reaction,[90,91] we next examined how bacterial responses were altered under iron depleted conditions. To this end, bacterial strains were treated with Tc in the presence of 2,2'-dipyridyl, an iron chelator.[76] As shown in Fig. 1.8G-L, bacterial strains remained viable under iron-deficient conditions after being treated with as high as 50 μg/ml Tc for 4 hrs (Fig. 1.8J-L). Again, two antibiotic-vulnerable mutants and exponential phase N16961 cells were completely killed by the same treatment in iron-sufficient LB media. We then examined whether bacterial killing was alleviated by co-treatment with N-acetyl cysteine (NAC), an ROS scavenger. Bacterial survival was substantially restored when antibiotic-sensitive (p)ppGpp^0 and Δ*dksA* mutants were co-treated with 5 mM NAC (Fig. 1.9B and C). As expected, NAC treatment exerted no protective effects on stationary phase N16961 cells already resistant to Tc treatment (Fig. 1.9A). Together, these results indicated that (i) iron availability determined bacterial survival during antibiotic stress and (ii) ROS, produced aerobically during antibiotic treatment, were responsible for bacterial killing.

Consistent with these results, post-antibiotic ROS production was indeed increased in two antibiotic-sensitive mutants (Fig. 1.10). When treated with Tc for 1 hr, ROS-specific fluorescent signals increased ~100- and ~1,000-fold in (p)ppGpp^0 and Δ*dksA* mutant, respectively. In contrast, fluorescent signals increased only ~10-fold in stationary phase N16961 cells and (p)ppGpp-accumulating Δ*relA*Δ*spoT* mutant (Fig. 1.10). It is of particular importance that

post-antibiotic ROS production was not detected in the Δ*acnB* single and (p)ppGpp^{0}Δ*acnB* quadruple mutant (Fig. 1.10), thereby further demonstrating that the recovered antibiotic resistance by *acnB* gene deletion is associated with the lack of ROS production.

Recently, we reported a recombinant N16961 strain that harbored an *eKatE* gene encoding a robust catalase.[79] The *eKatE* gene is derived from a commensal *E. coli* strain and this strain was found to be resistant to 2 mM H_2O_2 concentration. This strain, when harvested at the exponential phase, developed clear resistance to Tc treatment. While the control N16961 strain perished completely during the same treatment, ~10^4 cells remained viable (Fig. 1.9D). This result further supports our finding that ROS resistance can help with antibiotic tolerance.

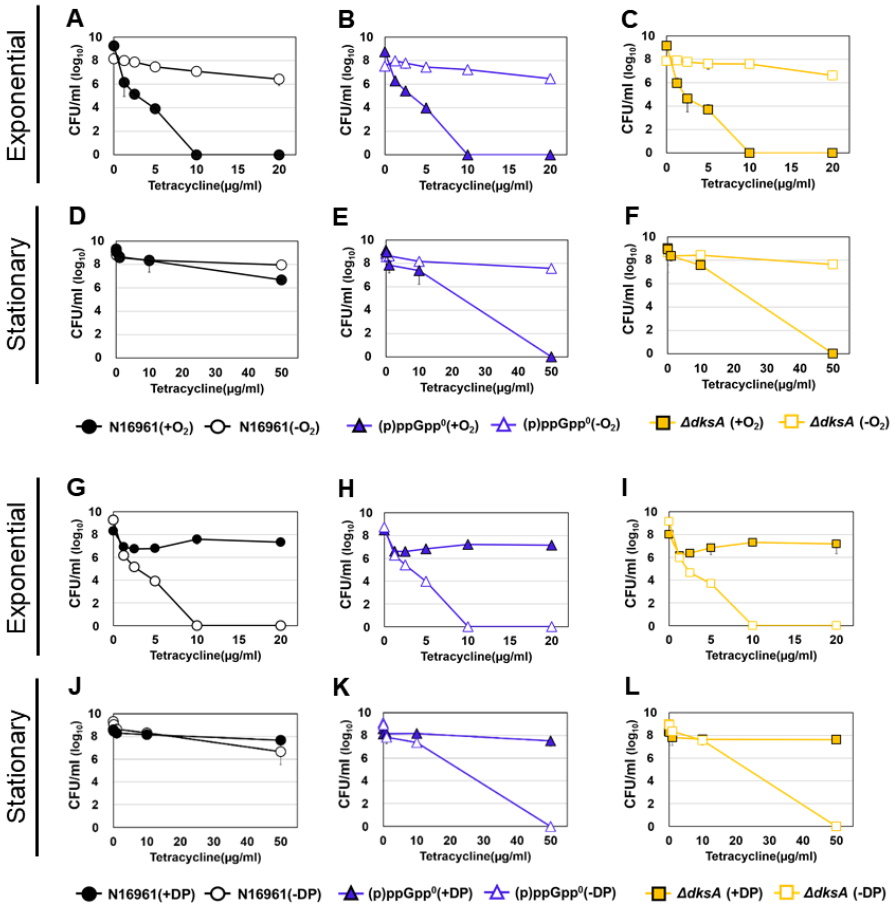

Figure 1.8. Recovery of tetracycline resistance of (p)ppGpp-deficient strains under anaerobic and iron-deplete conditions. (A-F) Tetracycline resistance of N16961 (circles), (p)ppGpp^0 mutant (triangles) and Δ*dksA* mutant (squares) strains under the anaerobic condition. Wild type N16961 and various (p)ppGpp-associated mutant strains were inoculated in LB and aerobically grown to each growth stage. Aliquots of each culture were resuspended in several concentrations of antibiotic containing LB broth and incubated for 4 hrs

in anaerobic condition. Each aliquot was sampled and 10-fold serially diluted to assess the number of CFU. (G-L) Tetracycline resistance of N16961 and (p)ppGpp-deficient mutant strains under iron-depleted condition. Aliquots of each culture were resuspended in several concentrations of tetracycline containing LB supplemented with 2,2'-dipyridyl and sampled at 4 hr post-inoculation and serially diluted for CFU counting.

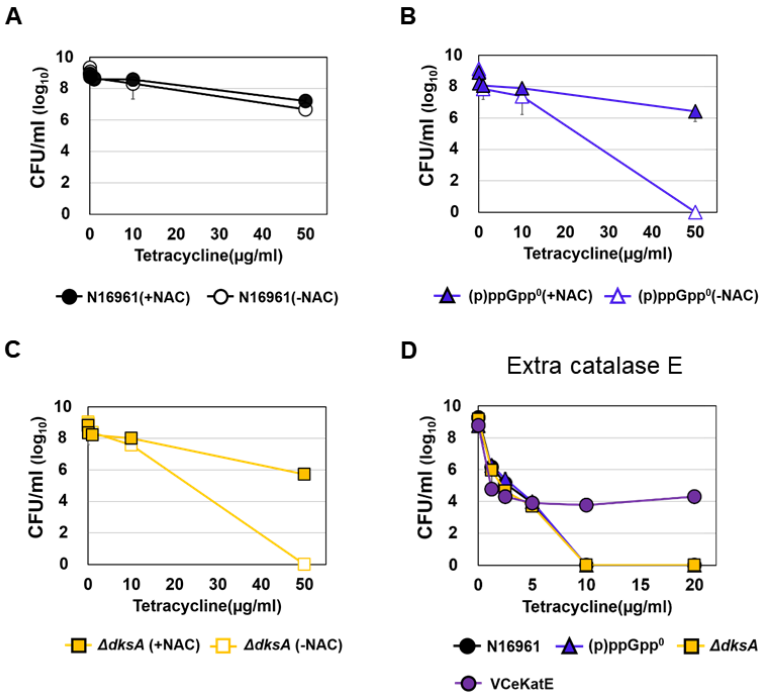

Figure 1.9. Effects of an ROS scavenger and additional catalase production on bacterial tetracycline resistance. (A-C) Tetracycline resistance of N16961 and (p)ppGpp-deficient mutant strains under ROS-scavenger treatment. Aliquots of each culture were resuspended in several concentrations of tetracycline containing LB supplemented with 5mM NAC, respectively and sampled at 4 hr post-inoculation and serially diluted for CFU counting. (D) Bacterial viability of (p)ppGpp-deficient mutants and eKatE-producing N16961 (N16961::pVIK112+*eKatE*) under the tetracycline treatment.

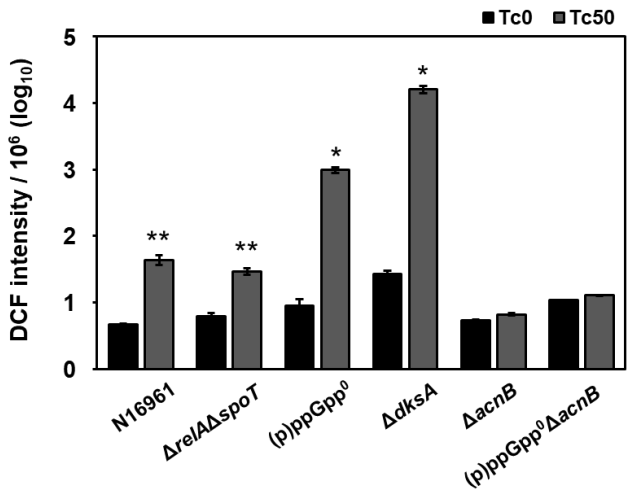

Figure 1.10. Antibiotic-induced ROS production in (p)ppGpp-deficient mutant strains. Bacterial strains indicated at the bottom were treated with 50 μg/ml Tc for 1 hr (gray bars) or left untreated (black bars). Following treatment, bacterial cells were stained with 50 μM DCF for 30 min to measure intracellular ROS levels. DCF intensity was normalized with bacterial CFU and is displayed in logarithmic scale. *, $p < 0.0001$ *versus* values of untreated groups. **, $p < 0.001$ *versus* values of untreated groups.

F. Larger amounts of intracellular free iron are present in SR-negative mutants

Next, we sought to further elucidate mechanisms by which (p)ppGpp regulates iron-dependent ROS production during aerobic antibiotic treatment. Table 1.3 lists the top 5 genes, expression of which was highly induced in the antibiotic-susceptible (p)ppGpp^0 mutant, as normalized with that of each counterpart in the antibiotic-tolerant Δ*relA*Δ*spoT* mutant. Among these are genes encoding heme transport protein (*hutA*), enterobactin receptor protein (*irgA*) and periplasmic iron (III) ABC transporter substrate-binding protein (*fbpA*). Because these proteins are involved in iron acquisition, these RNASeq data strongly suggest that the iron uptake system may be inversely regulated by intracellular (p)ppGpp levels. Consistent with this notion, production of FbpA protein was markedly increased in two SR-negative mutants, while its production was not detected in the (p)ppGpp-accumulating Δ*relA*Δ*spoT* mutant (Fig. 1.11A).

To understand the role of FbpA in iron uptake and antibiotic tolerance, we introduced an in-frame deletion of *fbpA* gene in N16961, (p)ppGpp^0 and Δ*dksA* mutants. Bacterial growth was not affected by *fbpA* gene deletion (data not shown). When we measured intracellular free iron concentrations by whole-cell EPR spectrometry, iron-specific signals were invariably decreased in the N16961, (p)ppGpp^0 or Δ*dksA* strains when the *fbpA* gene was inactivated (Fig. 1.11B). The (p)ppGpp^{0}Δ*fbpA* quadruple and Δ*dksA*Δ*fbpA* double mutants

contained ~2-fold and ~3.3-fold decreased levels of free iron, respectively, when compared with their parental mutants (Fig. 1.11B). These results showed that FbpA protein played an important role in iron uptake in *V. cholerae*. It is of particular interest that substantially increased amounts of free iron were detected in two antibiotic-susceptible mutants, as compared with N16961 (Fig. 1.11B). Together, these results clearly demonstrated that the iron import system was suppressed by (p)ppGpp accumulation, and this downregulation could contribute to reducing the level of intracellular free iron, the crucial source of hydroxyl radical (OH·) formation.

In line with these findings, bacterial survival under Tc treatment was significantly increased in Δ*fbpA* mutants (Fig. 1.12A-F). When exponential phase cells were used for treatment, bacterial viability of up to ~10^4-fold was recovered in Δ*fbpA*, (p)ppGpp^{0}Δ*fbpA*, Δ*dksA*Δ*fbpA* mutants compared with each of their background strains (Fig. 8A, C, and E). Moreover, (p)ppGpp^{0}Δ*fbpA*, Δ*dksA*Δ*fbpA* mutants, harvested at the stationary stage, also exhibited Tc resistance (Fig. 8D and F).

Table 1.3. List of genes showing the expression significantly increased in (p)ppGpp^0 compared with Δ*relA*Δ*spoT* mutant

Gene No.	Δ*relA* Δ*spoT*	(p)ppGpp^0	(p)ppGpp^0 /Δ*relA*Δ*spoT*	Product
VCA0819	129.41	2612.98	20.19	Co-chaperonin GroES
VC2664	217.95	3203.18	14.70	Molecular chaperone GroEL
VCA0576	134.48	1804.06	13.42	Heme transport protein HutA
VC0475	101.92	1343.82	13.19	Enterobactin receptor protein IrgA
VC0608	219.09	2653.88	12.11	iron (III) ABC transporter substrate-binding protein FbpA

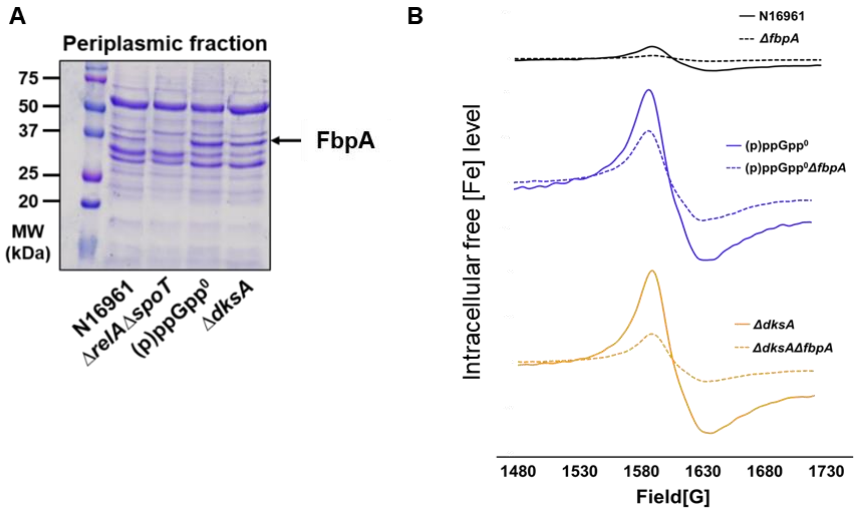

Figure 1.11. SDS PAGE analysis of periplasmic proteins and electron paramagnetic resonance (EPR) analysis to measure intracellular iron concentration. (A) SDS-PAGE analysis of periplasmic fractions in wild type and (p)ppGpp-associated mutants. Periplasmic fraction was extracted at 16 hr from bacterial cells grown under LB and loaded onto SDS-PAGE. (B) The levels of intracellular unincorporated iron in N16961 and (p)ppGpp-deficient mutant and *fbpA*-deletion mutant strains were measured by whole-cell electron paramagnetic resonance (EPR) analysis. The EPR peaks represent the content of total free iron converted to ferric form.

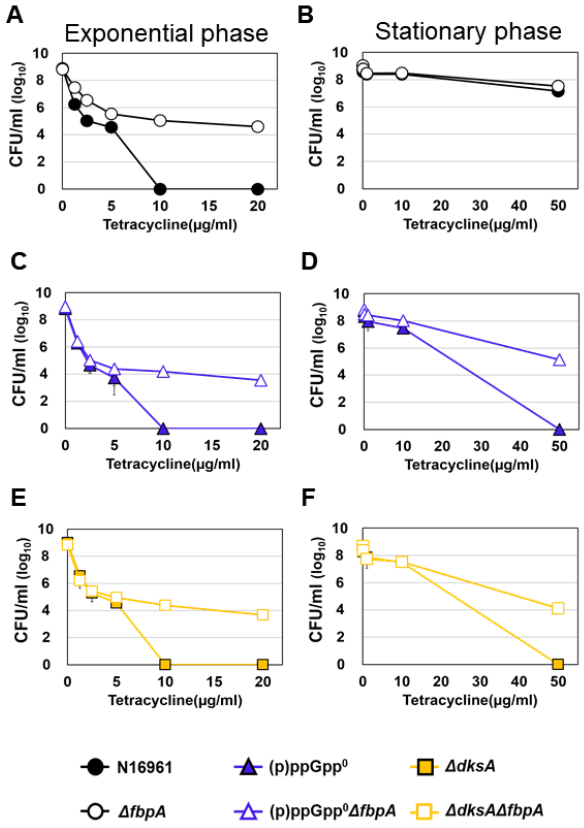

Figure 1.12. Effects of *fbpA* gene deletion on tetracycline resistance. (A-F) Bacterial viability of the (p)ppGpp-deficient mutant and *fbpA*-deletion mutants under tetracycline treatment. Aliquots of each culture were resuspended in several concentrations of antibiotic containing LB broth and sampled at 4 hr post-inoculation and serially diluted for CFU counting.

4. DISCUSSION

Cholera is characterized by CT-induced profuse watery diarrhea. Rapid loss of body fluids often leads to fatal dehydration.[24,92,93] Although up to 80% of cholera patients can be treated with oral rehydration therapy (ORT), annual deaths up to 120,000 are reported (WHO, 2014). Mortality includes victims who fail to receive immediate interventions and young patients with immature stomach function (WHO, 2012). These cases apparently need prompt antibiotic treatment to reduce the volume of diarrhea and kill the causative pathogen, *V. cholerae*. Treating cholera patients with antibiotics, however, has been a challenge due to the increased emergence of antibiotic-tolerant *V. cholerae* strains.[59-63,94]

In this study, we proposed that stringent response (SR), a conserved bacterial stress response mechanism, regulates antibiotic tolerance in *V. cholerae* via mechanisms that eventually suppress ROS production. SR controls metabolic activity and intracellular iron level, both of which affect bacterial growth and thereby antibiotic-induced ROS generation. Our successful demonstration on this important issue was made possible by the availability of the Δ*relA*Δ*spoT* double mutant that spontaneously accumulates intracellular (p)ppGpp. While (p)ppGpp null phenotypes have been well documented in various bacterial species,[18,19,95,96] cellular phenotypes induced by natural (p)ppGpp accumulation have not been clearly described. The (p)ppGpp-accumulating Δ*relA*Δ*spoT* mutant (i) metabolized slowly, (ii) exhibited a smaller cell-size phenotype and

(iii) produced significantly decreased levels of FbpA protein involved in iron acquisition. All of these phenotypes were invariably reversed in (p)ppGpp^0 and Δ*dksA* mutants, determined to be antibiotic-susceptible. Among these phenotypes, FbpA-mediated iron metabolism provided us with a clue that helped us precisely elucidate the role of ROS in antibiotic-mediated bacterial killing.

V. cholerae is an enteric pathogen that is transmitted through the fecal-oral route. The toxigenic *V. cholerae* is able to rapidly spread through bacterial shedding by evoking deadly diarrhea. It passes through the esophagus and comes into contact with the acid environment of the stomach, to which *V. cholerae* is known to be susceptible. Moreover, *V. cholerae* colonizes the small intestine, where it must compete with diverse species of commensal microbes for nutrients.[97] To overcome such unfavorable conditions, it is highly likely that SR is activated in *V. cholerae* inside the host intestine. Consistent with this idea, our previous work[19] demonstrated that (i) SR-defective mutants are incapable of colonizing mouse intestine and (ii) the (p)ppGpp-accumulating Δ*relA*Δ*spoT* mutant produces a markedly increased level of CT. We therefore proposed that strains that survive and shed out to the environments may have active SR and thereby be more able to infect subsequent hosts and overcome antibiotic stresses. To further validate this hypothesis, it will be important to compare SR activity status in pandemic vs. non-virulent environmental strains.

Our results demonstrated that (p)ppGpp, when accumulated, downregulated

expression of many TCA cycle genes including *acnB*. Not surprisingly, bacterial metabolism and growth were reported to be suppressed by SR in diverse bacterial species.[64,98,99] Studies also suggested that (p)ppGpp-mediated regulation participated in bacterial persister formations by mechanisms that involved toxin-antitoxin modules.[100,101] Bacterial persisters are transient phenotypic variants that are stochastically induced within a subset of cells in a given population.[101] Persister cells, in general, are more tolerant of antibiotic treatments.[102] Ronayne and colleagues showed that *E. coli* cells undergo cell elongation during the acquisition of a persister phenotype.[88] In contrast, *V. cholerae* cells, incubated for a long time in nutrient-poor media, were shown to be smaller in size when compared to normal state cells,[35] suggesting that the potential persister-like phenotype may be achieved in a distinct manner in *V. cholerae*. Our results showed that the (p)ppGpp-accumulating Δ*relA*Δ*spoT* mutant and SHX-treated N16961 cells were thinner and shorter. Interestingly, reduced cell size was also observed in the Δ*acnB* single mutant. These results indicated that cell shape change and a resultant increase in antibiotic tolerance ensued from (p)ppGpp accumulation or *acnB* gene deletion in *V. cholerae* and presented a new question as to which of these two cellular processes was the primary cause of the phenotype. Because a similar cell-size reduction was also detected in the (p)ppGpp^0*ΔacnB* mutant cells, we postulate that *acnB* gene deletion is a necessary and sufficient condition for the phenotype. Likewise, cell size reduction in the Δ*relA*Δ*spoT* mutant was likely induced by suppressed

aconitase activity, not directly by (p)ppGpp accumulation. Cell biological features need to be further explored in terms of how inactive metabolism can lead to changes in cell shape.

Periplasmic iron (III) ABC transporter substrate-binding protein, encoded by *fbpA*, was highly produced in antibiotic-susceptible (p)ppGpp^0 and Δ*dksA* mutants. More importantly, EPR analysis clearly showed that intracellular free iron was concomitantly increased in these two mutants. Like other bacterial species, *V. cholerae* requires iron for growth and possesses a variety of iron uptake systems.[103] The iron acquisition systems in *V. cholerae* involve synthesis, secretion and uptake of a range of siderophore molecules, such as vibriobactin[104], enterobactin[105,106] and ferrichrome[104,107]. In addition, *V. cholerae* possesses *feo* and *fbp* gene clusters encoding systems for the acquisition of ferrous and ferric iron, respectively.[103] The Fbp system is a periplasmic binding protein-dependent ABC transport system and consists of three genes, *fbpA* (VC0608), *fbpB* (VC0609), and *fbpC* (VC0610). The *fbpB* and *fbpC* encode membrane-spanning proteins forming a pore across the cell membrane and ATP binding proteins, respectively. The *fbpA* encodes a substrate-binding protein that carries ferric iron to the membrane-spanning proteins. Studies indicate that the potential Fur box (ferric uptake regulator binding motif) exists in the promoter region of the *fbpABC* operon,[103,108] suggesting that expression of the operon is highly induced under iron-deficient conditions. However, in our experiments, bacterial strains were grown in LB,

considered to be a nutrient-rich media. It was of particular interest to us that the Fur protein is inactivated by the presence of ROS.[109] ROS oxidizes Fe^{2+}, a co-factor of Fur, converting active Fur into an inactive apo-form. Therefore, one possible explanation for the antibiotic-mediated bacterial killing in the antibiotic-susceptible (p)ppGpp^0 and Δ*dksA* mutants would be that ROS produced during de-repressed aerobic growth stimulated FbpA-mediated iron uptake, which in turn amplified further ROS production. In support of this idea, the Δ*relA*Δ*spoT* mutant that grew very slowly produced undetectable levels of FbpA protein. Furthermore, we also found that FbpA production was reduced in the Δ*acnB* mutant that exhibited a slow growth phenotype (data not shown).

In our experiments, the first-line drugs for treating cholera patients, tetracycline, erythromycin and chloramphenicol, were used. We found that SR-deficient mutants of *V. cholerae* completely lost their viability as the antibiotic concentration increased. Interestingly, however, the antibiotics that turned out to be very effective at killing *V. cholerae* strains are commonly known as bacteriostatic. Although it is still debatable how to classify antibiotics as bacteriostatic or bactericidal based on their *in vitro* test results, recent studies described their differences based on their effects on bacterial metabolism. Lobritz and colleagues found that bacteriostatic and bactericidal have opposing effects on bacterial respiration in *E. coli* and *Staphylococcus aureus.*[77] They demonstrated that bacteriostatic antibiotics, such as tetracycline, chloramphenicol and erythromycin, decelerate cellular respiration, whereas

bactericidal antibiotics accelerate basal respiration and lead to producing ROS as a by-product. On the other hand, we found that bacteriostatic antibiotics killed bacteria and produced deleterious ROS. Interestingly, in another study the antibiotics which did not trigger SOS responses in *E. coli* caused SOS responses in *V. cholerae*.[110] SOS stress responses were activated when exogenous and endogenous triggers provoked DNA damage, and some antibiotics act as exogenous triggers that stimulate ROS production, the crucial weapon of DNA disruption. Aminoglycosides, tetracycline and chloramphenicol induce SOS responses in *V. cholerae*, unlike *E. coli*, and this result suggests the possibility that these antibiotics have more deleterious effects on *V. cholerae*. Taken together, our results suggest that effects of bacteriostatic and bactericidal antibiotics on bacteria vary from species to species.

In conclusion, our results revealed that bacterial SR regulates antibiotic tolerance by modulating ROS production. Central metabolism and iron transport systems are subject to (p)ppGpp-mediated regulation (summarized in Fig. 1.13). When (p)ppGpp is accumulated, the TCA cycle is downregulated to slow down bacterial growth. At the same time, FbpA-mediated iron uptake is also suppressed in (p)ppGpp-accumulating cells. These dual cellular events both contribute to physiological changes resulting in metabolic slowdown and therefore antibiotic-tolerant states. Bacterial SR has been a target to be inhibited. Chemical compounds that can suppress (p)ppGpp production, such as relacin[111]

and iMAC[45] can potentially be used as antibiotic adjuvants. We anticipate that experimental data provided in the current study will stimulate future investigations that eventually help us come up with better strategies to combat bacterial infections, including one by the deadly enteric pathogen, *V. cholerae*.

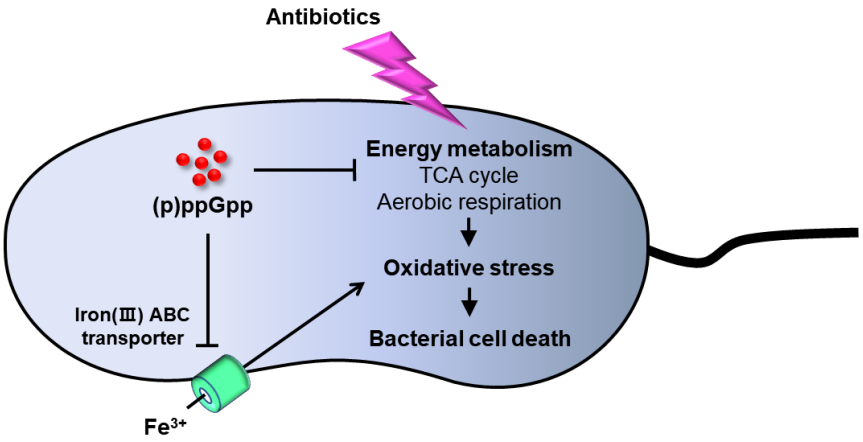

Figure 1.13. Summary of (p)ppGpp-mediated regulation of antibiotic resistance in *V. cholerae*. Antibiotic treatment stimulates ROS production by hyperactivating bacterial central metabolism. The released ROS leads to damage of intracellular DNA, proteins, and lipids, which results in cell death. However, (p)ppGpp negatively regulates TCA cycle and aerobic respiration. The downregulation of aerobic respiration can reduce oxidative stress and eventually prevent cell death. The (p)ppGpp can maximize this effect by restricting free iron uptake from the iron transporting system.

Chapter III. Two Distinct Stringent Response Alarmones Induce Physiologically Separated Phenotypes in *Vibrio cholerae*

1. INTRODUCTION

As bacteria often encounter a variety of unfavorable environmental stresses such as nutrient starvation, they utilize a cascade sensory system consisting of various secondary messenger molecules to monitor the external stimuli.[8,9] These molecules force bacteria into a growth-arrested state while they rearrange the bacterial metabolic systems in order to promote adaptation to stressful conditions.

(p)ppGpp (guanosine penta-phosphate or tetra-phosphate), also known as the mediator of stringent response (SR), systematically modifies bacterial physiology when the bacteria face stresses.[6] Upon exposure to several stresses, (p)ppGpp delays bacterial growth by inhibiting the production of ribosomal RNA,[1] which allows transcriptional reprogramming with the cooperation of RNA polymerase. (p)ppGpp is produced when pyrophosphate of ATP is added to either GDP or GTP.[6,8,9] The intracellular concentration of (p)ppGpp is mainly controlled by RelA and SpoT protein in most Gram-negative bacteria.[6,8,9] These two enzymes are long-RSH (RelA/SpoT Homologue) consisting of a hydrolase (HD) and a synthetase (SYNTH) domain in the N-terminal and a regulatory domain in the C-terminal domain.[6] RelA, a mono-functional synthetase lacking

the HD domain, can produce (p)ppGpp upon amino acid starvation. (1)The initiation of (p)ppGpp synthesis during amino acid depletion occurs when the accumulated uncharged tRNAs in bacterial cytoplasm signals RelA to bind deacetylated tRNA on vacant ribosomal A site.[6,7] When uncharged tRNAs accumulate in bacterial cytoplasm, RelA readily recruits deacetylated tRNA to the vacant ribosomal A site, initiating the synthesis of (p)ppGpp.[7] On the contrary, SpoT signals the synthesis of (p)ppGpp via a non-ribosomal associated reaction, bearing additional stresses such as fatty acid or carbon starvation.[10,11] The versatile roles of SpoT in stress response are attributes of both active HD and SYNTH domain, making it a bifunctional enzyme.[112]

Although long RSH protein is the main enzyme responsible for SR activity, some bacteria also possess genes encoding short-RSH, SAS (small alarmone synthetase) and SAH (small alarmone hydrolase), lacking the regulatory domain.[6] Single-domain RSHs are commonly found in Gram-positive bacteria, which might exist for sensing sources of environmental stresses other than amino acid starvation recognized mostly by long-RSHs. For example, transcription of *relP* and *relQ* encoding for two SASs in *Bacillus subtilis* is upregulated against the stresses on the cellular envelope[113-115] and the shock by the presence of alkaline.[115,116] When expressed, SASs construct the homo-tetrameric structure for synthesizing (p)ppGpp to cope with the stresses.[117]

Nevertheless, the question on why some Gram-negative bacteria carry the SASs and / or SAHs from evolutionary aspects remains unresolved. SASs and

SAHs are very multifarious that they can belong to many different subfamilies and moreover, there might be some additional unknown proteins playing potential roles in nucleotide alarmone synthesis. Recent studies have provided a new insight into RSH, suggesting the novel role of SASs acting as a toxin itself beyond an upstream regulator of SR.[118,119] The potential of SAS toxicity was described in earlier research demonstrating that overproduction of (p)ppGpp molecules derived by RelA resulted in the alarmone becoming toxic to bacterial growth, when it is not counteracted by SpoT.[118]

The toxic SAS (toxSAS) was first discovered in a gene cluster derived from mycobacterial prophage.[119] gp29, a viral defense protein including a partial RSH domain, was exceedingly toxic to *Mycobacterium smegmatis* itself. The toxicity was neutralized by the co-expression of its neighboring gene gp30, a proposed immunity of gp29. Recent research revealed that the type-6 secretion system (T6SS) toxic effector protein, Tas1, had a homologous domain with RSH by producing (p)ppApp (adenosine penta- or tetra-phosphate) instead of (p)ppGpp in the virulent *Pseudomonas aeruginosa* strain PA14.[120] In addition, Ahmad and his colleagues found that *E. coli* undergoing Tas1 intoxication displayed a dramatic loss of viability unlike that RelA overexpression.[120] This interbacterial toxin has an immunity protein placed right after the downstream of its gene loci, and the toxic effect is directed to another cell by a T6SS.

The activities of toxSAS proteins, gp29 and Tas1, are known to be regulated by their inhibitor proteins.[119,120] Recently, Jimmy and his colleagues discovered

that in many bacteria, SASs encoding genes are structured as an operon architecture together with immunity proteins resembling a toxin-antitoxin (TA) module due to the inherent toxic effects.[121] They updated a new genetic database of potential RSH domain from widespread species and constructed a phylogenetic tree using their computational tools. They validated the toxicity of SAS proteins characterized by TA loci and found that toxSASs exert their toxicity through the production of nucleotide alarmones, (p)ppGpp or (p)ppApp. And its neighboring partner located downstream or upstream of the toxin gene acts as a type II or type IV antitoxin for diminishing the SAS-mediated toxicity.

Vibrio cholerae, the causative pathogen of cholera, induces severe diarrheal symptom in the host environmental niche.[21,22] From previous studies, we found that SR had a canonical role for survival fitness of *V. cholerae*.[19,40,41] Unusually, although SASs are rarely discovered in Gram-negative bacteria, *V. cholerae* has an additional unique SAS protein, RelV.[42] RelV was first discovered from a suppressor mutant of Δ*relA*Δ*spoT* strain, exhibiting a (p)ppGpp^0 phenotype.[65] In contrast to RelA, RelV was reported not responding to amino acid starvation, but producing (p)ppGpp under glucose depletion.[42] In our previous research, we uncovered that cholera toxin production under anaerobic TMAO respiration was significantly increased by SR.[19] Interestingly, we observed that RelV plays more crucial role in CT production compared to RelA from the experiment. To date, although the relationship between SR and cholera phenotypes has been widely studied in many research groups, the actual role of each SR enzyme,

especially RelV, in *V. cholerae* SR remains unclear.

In this study, we investigated a bona fide function of RelV, which has never been fully illustrated. We described the distinctive physiology of *V. cholerae* under the state on which its RelV enzyme was overproduced by comparing to the RelA expression. Interestingly, we discovered that high concentration of RelV perishes *V. cholerae* itself by producing the toxic nucleotide products, while RelA and its collateral products just arrest the bacterial growth and sustain viability. Additionally, we elucidated that each RSH enzyme in *V. cholerae* has distinct regulons which affect bacterial virulence, respectively. This report suggests a novel insight about *V. cholerae* SR enzymes, especially RelV and furthermore, uncovered its toxic products that contributes to global bacterial physiology.

2. MATERIALS AND METHODS

A. Bacterial strains and growth conditions

All bacterial strains and plasmids used in this study are listed in Table 2.1. Bacterial cultures were grown in Luria-Bertani medium (LB; 1% (w/v) tryptone, 0.5% (w/v) yeast extract, and 1% (w/v) sodium chloride) at 37 °C, and antibiotics were used according to the following concentrations: streptomycin (Duchefa), 200 μg/ml; ampicillin (Sigma), 100 μg/ml; and kanamycin (Duchefa) 50 μg/ml. All bacterial single colonies on LB plates were picked and inoculated in LB broth for precultures. Precultures were diluted to OD_{600} 0.02 in fresh LB broth for subculture and incubated at 37 °C with shaking. The incubation period was dependent on experimental procedures.

Table 2.1. Bacterial strains and plasmid used in this study

Strains or plasmids	Relevant characteristic	Source
***V. cholerae* strains**		
N16961	Wild type, O1 serogroup, biotype El Tor	Lab collection
(p)ppGpp^0	N16961, *relA*, *relV* and *spoT* deleted	[19]
Δ*relA*Δ*relV*Δ*VC1223*Δ*spoT*	N16961, *relA*, *relV*, *VC1223* and *spoT* deleted	This study
***E. coli* strains**		
BL21 (DE3)		Lab collection
Plasmids		
pBAD24	Amp^r, cloning vector	Lab collection
pBAD24::*relA*-his	Amp^r, RelA overexpression vector	This study
pBAD24::*relV*-his	Amp^r, RelV overexpression vector	This study
pBAD24::*relV-VC1223*	Amp^r, RelV-VC1223 overexpression vector	This study
pBAD24::*spoT*-his	Amp^r, SpoT overexpression vector	This study
pBAD24::*VC1223*	Amp^r, VC1223 overexpression vector	This study
pCVD442	Amp^r, *sacB* suicide vector from plasmid pUM24	Lab collection
pCVD442::*relA*-flanking	Amp^r, suicide vector for *relA* deletion	This study
pCVD442::*relV*-flanking	Amp^r, suicide vector for *relV* deletion	This study
pCVD442::*spoT*-flanking	Amp^r, suicide vector for *spoT* deletion	This study
pCVD442::*VC1223*-flanking	Amp^r, suicide vector for *VC1223* deletion	This study

B. Construction of in-frame deletion mutants

V. cholerae mutants were created via allele exchange, as previously described with a few modifications.[41] To induce mutation, about 500bp flanking sequences located at both ends of the ORF and whole linear sequences of pCVD442 were amplified by PCR with primers listed in Table 2.2. The primers carried anchor sequences where vector and flanking regions overlap each other. The purified flanking sequences and vector were both ligated with Gibson assembly master mix (E2621, NEB). ligates were then transformed to heat-shock competent cells; DH5α/λ pir strains. Cloning vectors were purified from the viable transformed cells screened from LB plates containing 100 μg/ml ampicillin. The cloned vectors underwent an additional transformation to yield SM10/λ pir strains. The SM10/λ pir strains harboring recombination vectors was mixed thoroughly with *V. cholerae* recipient strains in a ratio of 3:1, respectively. The mixture was spread onto LB plates and incubated for 6 hrs at 37 °C. For the first step in allelic exchange, the mixed pool was suspended in fresh LB broth and spread onto LB plates containing both streptomycin 200 μg/ml and ampicillin 100 μg/ml. Following the overnight culture, selected single colonies were streaked onto LB plates supplemented with 8% sucrose and streptomycin 200 μg/ml without the addition of NaCl, to excise plasmid from the chromosome by second cross-over. Screening of in-frame deletion sites for each colony was preceded by PCR to identify the desired allele with primers that contains flanking sequences and ORF.

Table 2.2. Primers used in this study

Gene name	Direction	Primer sequence (5'-3')
pBAD24/*relA* His-F1	F	ggaggaattcATGGTTGCGGTACGAAGC
pBAD24/*relA* His-R1	R	caaaacagcctcaatggtgaTGATGGTGATGACCTAAGCGTTTGACCAACA
pBAD24/*relA* His-vF1	F	tcaccattgaGGCTGTTTTGGCGGATGAG
pBAD24/*relA* His-vR1	R	ccgcaaccatGAATTCCTCCTGCTAGCC
pBAD24/*relV* His-F1	F	ggaggaattcATGAGTCTATTGCTACGTACCAC
pBAD24/*relV* His-R1	R	caaaacagcctcaatggtgaTGATGGTGATGTGCCGCTTGAATGTGCGTT
pBAD24/*relV* His-vF1	F	tcaccattgaGGCTGTTTTGGCGGATGAG
pBAD24/*relV* His-vR1	R	atagactcatGAATTCCTCCTGCTAGCC
pBAD24/*relV1223*-F1	F	ggaggaattcATGAGTCTATTGCTACGTAC
pBAD24/*relV1223*-R1	R	caaaacagccTCAAAGTCGAAAAATAAGACC
pBAD24/*relV1223*-vF1	F	tcgactttgaGGCTGTTTTGGCGGATGAG
pBAD24/*relV1223*-vR1	R	atagactcatGAATTCCTCCTGCTAGCC
pBAD24/*spoT* His-F1	F	ggaggaattcttgtatCTATTCGATAGTCTAAAAGACGTTGCC
pBAD24/*spoT* His-R1	R	caaaacagcctcaatggtgaTGATGGTGATGGTTCTTACGGCGGCGCACTT
pBAD24/*spoT* His-vF1	F	tcaccattgaGGCTGTTTTGGCGGATGAG
pBAD24/*spoT* His-vR1	R	atagatacaaGAATTCCTCCTGCTAGCC
pBAD24/*VC1223*-vF1	F	tgggctagcaggaggaattcATGCGCAAATTGCCAAGATG
pBAD24/*VC1223*-vR1	R	GAATTCCTCCTGCTAGCC
pCVD442-vF1	F	GCATGCGGTACCTCTAGAAG
pCVD442-vR1	R	GAGCTCTCCCGGGAATTC
pCVD/*relA*-UP-F1	F	tggaattcccgggagagctcCTTCGCAAAACCAACTAAC
pCVD/*relA*-UP-R1	R	gttggatttaATTGATATCGTCCTAATAATTGTATTTTTAG
pCVD/*relA*-DW-F1	F	cgatatcaatTAAATCCAACGCAAACAGC

pCVD/*relA*-DW-R1	R	cttctagaggtaccgcatgcGATCGCCTAGCTC TTCCTC
pCVD/*relV*-UP-F1	F	tggaattcccgggagagctcGCAAAGAAAGA ACGTACC
pCVD/*relV*-UP-R1	R	gatctgctcaCACTCTCCTTAGCTTGCG
pCVD/*relV*-DW-F1	F	aaggagagtgTGAGCAGATCCAAACCAT TG
pCVD/*relV*-DW-R1	R	cttctagaggtaccgcatgcTCAGAAGGTTGG CATACAC
pCVD/*spoT*-UP-F1	F	tggaattcccgggagagctcAATCCGTAGCCA AATGCCAG
pCVD/*spoT*-UP-R1	R	accttggcggGGCCCGGCGGGTTAAATC
pCVD/*spoT*-DW-F1	F	ccgccgggccCCGCCAAGGTGCATTGGC
pCVD/*spoT*-DW-R1	R	cttctagaggtaccgcatgcTCTAAGCCTTGAT TACCGCGTTTG
pCVD/*VC1223*-UP-F1	F	gggagagctcCACCAATTCAACGGAAGA TAAC
pCVD/*VC1223*-UP-R1	R	gagaacatcaTTATGCCGCTTGAATGTG
pCVD/*VC1223*-DW-F1	F	agcggcataaTGATGTTCTCGACACGGG
pCVD/*VC1223*-DW-R1	R	taccgcatgcAAATCAGATGAAAACAGG CTC

C. Detection of intracellular (p)ppNpps' spots by TLC

Two-dimensional TLC for detecting (p)ppNpps' spots was performed as previously described with a few modifications.[122] Briefly, all bacterial strains were grown aerobically with the supplementation of 100 μCi/ml [^{32}P] orthophosphate (PerkinElmer Life Sciences). The bacterial cell pellets were recruited at each time point and resuspended in a 10 mM Tris-HCl buffer (pH 8.0). After the equal addition of 26.3M formic acid, freeze-thaw cycling was performed in liquid nitrogen. The cell debris-free supernatants collected after centrifugation were spotted onto 20 cm x 20 cm PEI-cellulose F TLC plates (Merck). For the one-dimensional separation, TLC plates were developed in 1 M LiCl and 4 M formic acid buffer. This step was followed by soaking plates in methanol for 15 min and a two-dimensional run in 0.85 M KH_2PO_4 buffer (unadjusted pH). Autoradiograms were visualized using phosphorimager (Typhoon 7000, GE Healthcare).

D. Confocal microscopy

Confocal microscopy was conducted according to the manual description of FV-1000 (Olympus Optical Co. Ltd., Japan). Aliquots of each culture were stained with Syto-9 and Fm4-64 for the cellular morphology comparison of *V. cholerae* including DNA and cell membrane. To capture the green and red fluorescence, samples were examined at 488 and 594 nm wavelengths, respectively.[123] Both DIC and each fluorescent image were collected simultaneously.

E. Scanning electron microscopy analysis

Characterizations of bacterial cell morphologies were performed via visualization under scanning electron microscopy, following the procedures previously described.[41] In short, bacterial cell cultures were fixed with PBS containing 2% glutaraldehyde and 0.1% paraformaldehyde and stained with 1% OsO_4. Then, they were coated with Platinum by an ion sputter (Leica EM ACE600) and examined with a field emission scanning electron microscope (Merlin, Zeiss, Germany) at an acceleration voltage of 20 kV.

F. RNA-sequencing analysis

Bacterial cultures grown in LB were harvested at 30 min post 0.1% arabinose induction. Each bacterial culture sample was duplicated for RNA analysis. To extract high quality bacterial RNA, a RNeasy Protect kit (Qiagen) was used with a RNeasy mini kit (Qiagen) following the manufacturer's protocol. The quantity and the quality of total RNA were evaluated using RNA electropherograms (Agilent 2100 Bioanalyzer; Agilent Technologies, Waldbroon, Germany) and ND-2000 Spectrophotometer (Thermo Inc., DE, USA), respectively. To control and test RNAs, rRNA was removed using NEBNext rRNA Depletion Kit (Bacteria) from the RNA samples each containing 5 ug of total RNA. The library construction was performed using NEBNext Ultra II RNA Library Prep Kit according to the manufacturer's instructions. The rRNA-free RNAs were used for cDNA synthesis and shearing, following manufacturer's instruction. Indexing was performed using Illumina

indexes 1-12. The enrichment step was carried out using PCR. Subsequently, libraries were checked using Agilent 2100 bioanalyzer (DNA High Sensitivity Kit) to evaluate the mean fragment size. Quantification was performed with the library quantification kit using a StepOne Real-Time PCR System (Life Technologies, Inc., USA). High Throughput sequencing was performed as paired-end 100 sequencing using HiSeq 2500 (Illumina, Inc., USA). Bacterial-Seq reads were mapped by Bowtie2 software tool in order to obtain the alignment file. Differentially expressed genes were determined based on the counts from unique and multiple alignments using EdgeR within R (R development Core Team, 2016) using Bioconductor (Gentleman et al.,2004). The alignment file was also used for assembling the transcripts. Quantile normalization method was used for comparison between samples. Gene classification was based on searches conducted by DAVID.

G. Biofilm analysis

Biofilm assay was prepared according to the procedure described by Min and his colleague.[124] The overnight seed-culture of *V. cholerae* was inoculated in LB broth to OD_{600} ~0.02 and incubated aerobically at 37 °C with shaking at 220 rpm. At OD_{600} ~0.1, 0.1% arabinose was added and then dispensed to confocal dishes by volume of 3.5ml. Each bacterial culture was statically incubated for 24 hrs. Planktonic bacteria was primarily eliminated by flicking and washed with PBS for three times as a following step. Biofilm culture on the slide dishes was stained with 0.05% Syto9 (Invitrogen) and examined at 488 nm.

H. Swimming motility assay

Swimming assay was performed to measure the bacterial cell motility as described previously.[39] Bacterial cells were grown statically by spot-inoculation on 0.3% (w/v) agar LB plates supplemented with 100 μg/ml ampicillin and 0.1% arabinose. To estimate swimming motility, the diameter of the circular halo was measured after 12 hrs incubation at 30 °C.

I. Western blot analysis of cholera toxin

Western blot analysis for cholera toxin detection was performed as previously described.[84] Bacterial cells were grown anaerobically in LB-TMAO media (containing 50 μM TMAO) at 37 °C. 0.1% arabinose solution was treated at the early exponential phase where the turbidity of the bacterial culture was nearly OD_{600}=0.05. For western blot analysis, bacterial supernatants from each timepoint were concentrated by trichloroacetic acid (TCA, sigma). Rabbit polyclonal antibody raised against CT subunit B (Abcam Inc.) was used for target detection.

J. Statistical analysis

The data are expressed as the means ± S.D. Unpaired Student's t tests (two-tailed, unequal variance) were used to analyze the differences between experimental groups. p values < 0.05 were considered statistically significant. All experiments were repeated for reproducibility.

3. RESULTS

A. A small alarmone synthetase RelV possesses high homology to the Tas1 toxin domain of *Pseudomonas aeruginosa* PA14

The stress alarmone (p)ppGpp responds to the extracellular stresses which hinder cell proliferation such as bacterial growth and viability. (p)ppGpp enables bacteria to overcome unfavorable conditions by rearranging diverse bacterial metabolic systems. Recently, a novel RSH protein Tas1, which produces (p)ppApp and not (p)ppGpp, was discovered in PA14 strain of *P. aeruginosa.*[120] As an effector protein of T6SS, Tas1 utilizes the mechanistic dispatching of (p)ppApp to prey cells in order to lower their intracellular ATP levels and eventually cause cell death.

It was an unprecedented finding that the Tas1 toxin domain, a weak RSH homologue, produces a toxic nucleotide derivative to kill the neighboring bacterial cells. To determine whether Tas1 homologue exists in *V. cholerae*, we searched for a *V. cholerae* N16961 genome using the nucleotide sequence of *tas1* toxin domain as a query. Interestingly, we found that the relV gene of *V. cholerae* has a sequence homology to the query sequence (Fig. 2.1A). It was already well-known that RelV, a conserved SAS in *V. cholerae,* synthesizes (p)ppGpp as its products. Therefore, the similarity between RelV and Tas1 protein was unexpected. Although the entire sequence similarity is somewhat low (27%), RelV has an important catalytic glutamate residue conserved in Tas1 toxin domain. Moreover, an additional open reading frame (VC1223)

exists right at the downstream of *relV* (VC1224), similar to the toxin-immunity encoding region of *tas1-tis1* (Fig. 2.1A). Unlike RelV, no distinct similarity was found between Tis1 and VC1223 protein sequences (data not shown). To determine whether RelV attains the identical functionality of Tas1 toxin domain, we predicted a folding structure of RelV and overlaid it to the predetermined structure of $Tas1_{tox}$-Tis1 complex (PDB code 6OX6). Remarkably, structural overlay of RelV with $Tas1_{tox}$ revealed a highly conserved three-dimensional positioning of residues that interact with the pyrophosphate donor, ATP (Fig. 2.1B). In a previous study, two α-helices in $Tas1_{tox}$ were rotated by approximately 30° relative to the equivalent helices in the Rel proteins in *Bacillus subtilis* or *Staphylococcus aureus*.[120] In contrast to Rel proteins, the angle between the two α-helices in RelV proteins is substantially identical to that in the $Tas1_{tox}$ crystal structure (Fig. 2.1B). Based on these structural characteristics, we hypothesized that the products synthesized by RelV will likely be (p)ppApp and not (p)ppGpp. To address this hypothesis, we first implemented a series of experiments to understand RelV- or RelA-induced phenotypes in bacterial growth. To begin with, we overexpressed each of the three *V. cholerae* SR genes, *relA*, *relV*, and *spoT* in *E. coli* BL21 strain. At an early-exponential stage, *E. coli* strains harboring each pBAD24-derived overexpression plasmids were spotted on both arabinose supplemented and non-supplemented LB plates following the serial dilution. Interestingly, *E. coli* cells exhibited different cell viability phenotypes, under RelA- and RelV-

overexpressing conditions (Fig. 2.2). While both strains lost their viabilities, when compared to pBAD24 control, RelV-overexpressor showed even more defected growth than that of RelA-overexpressing cells. (Fig. 2.2). Notably, this remarkable reduction by *relV* gene overexpression is slightly recovered up to 10-fold by co-expression with *VC1223*. On the other hand, *spoT* overexpression did not affect bacterial growth. Consequently, we postulated that RelA and RelV, which have been known as the (p)ppGpp producers, may induce different phenotypes. In particular, we found that RelV showed higher toxicity against bacterial viability than RelA. Hence, in this study, we have focused on elucidating the distinct functions of RelV in *V. cholerae*.

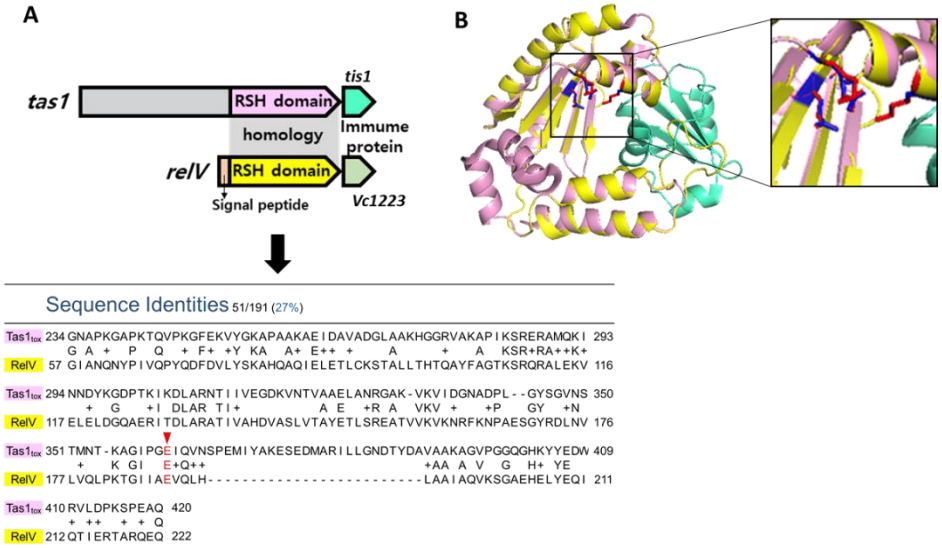

Figure 2.1. Genomic context and structural overlay of Tas1 of PA14 and RelV of N16961. (A) Genomic context of *tas1-tis1* and *relV* (*VC1224*)-*VC1223* of *P. aeruginosa* strain PA14 and *V. cholerae* N16961, respectively. (B) Structural overlay of $Tas1_{tox}$ (PDB code 6OX6) and the predicted modeling structure of RelV (SWISS modeling). $Tas1_{tox}$ and RelV structure are represented in pink and yellow, respectively as described in panel (A). The dotted box denotes the active site of Tas1 magnified on the right. The amino acids are shown as blue (Tas1)- or red (RelV)- sticks.

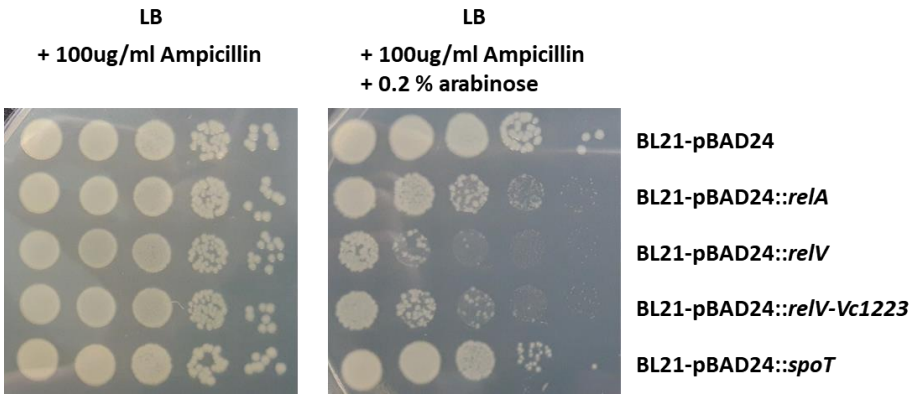

Figure 2.2. Bacterial CFU results of *E. coli* strains expressing *V. cholerae* SR enzymes. CFU plating of *E. coli* strain BL21 expressing the SR-enzymes of *V. cholerae*. Each BL21 strain carrying the plasmid was serially diluted when they reached an OD_{600} of 0.1 and spotted on LB-ampicillin plates with or without 0.2% arabinose.

B. Expression of *relA* or *relV* also exhibited different growth-associated phenotypes in *V. cholerae*

We discovered that overexpression of transformed *V. cholerae* SR enzymes in *E. coli* affected its growth in each different manner. To investigate the impact of overexpression of each gene in *V. cholerae*, we transformed a Δ*relA*Δ*relV*Δ*spoT* triple mutant of N16961, also known as (p)ppGpp^0 strain with the same set of plasmids. *V. cholerae* (p)ppGpp^0 strain carrying either pBAD24 control or pBAD24::*spoT* plasmid grew normally. In contrast, impaired growth was clearly observed when the expression of *relA* or *relV* gene was induced by arabinose. (Fig. 2.3A). After arabinose induction, *relA*-induced (p)ppGpp^0 mutants grew slowly and OD_{600} values were never increased. On the other hand, *relV*-overexpressor strain grew at a relatively normal rate though a substantial growth inhibition was observed in the beginning. (Fig. 2.3A). When live cells were enumerated by CFU counting, a definite difference between *relV*- and *relA*-overexpressors was revealed (Fig. 2.3B). Although (p)ppGpp^0 mutant harboring *relA* expression plasmid had few viable cells at the early time point of post-induction, the number of viable cells steadily increased over time (Fig. 2.3B). Following *relV* induction, however, (p)ppGpp^0 strain dramatically lost viabilities, resulting in a 1000-fold decrease in CFU over time (Fig. 2.3B). We were intrigued by the finding that no correlation existed between these two growth measurements. It was reported that (p)ppGpp- deficient *E. coli* strain displayed an elongated cellular morphotype, and this phenotype resulted in a

higher value of optical density.[125] We therefore observed cell shapes of each (p)ppGpp^0 strain using confocal microscopy. While both pBAD24 control and *spoT*-induced strain showed the typical comma-shaped *V. cholerae* cell shape, *relA*- or *relV*-overexpressor underwent significant alterations in cell morphology. (Fig. 2.4). The *relA*-overexpressed (p)ppGpp^0 mutant cells appeared as giant circular cells, resembling viable but nonculturable (VBNC) states of *Vibrio* species.[126] This specific phenotype accounts for the presence of fewer viable cells at initial state of growth in *relA*-inducing (p)ppGpp^0 strain (Fig. 2.3B). In addition, we also found small-sized bacterial cells in this group. On the other hand, *relV*-overexpressing (p)ppGpp^0 mutants represented abnormally elongated cell morphotypes (Fig. 2.3B). This unusual morphology of bacterial cells may result in a decrease in CFU as the culture progressed (Fig. 2.3B). Through the analysis of intracellular DNA and cell membrane staining, we suggested that the defection in cell division observed among the elongated cells results from the stretching of DNA without membrane partitioning (Fig. 2.4). Together, these results demonstrate that two proteins RelA and RelV introduce distinct growth-associated phenotypes, thereby suggesting that these alarmone synthetases may produce different products in *V. cholerae*. As was observed in *E. coli*, overexpression of *spoT* gene did not induce any noticeable changes in *V. cholerae* growth.

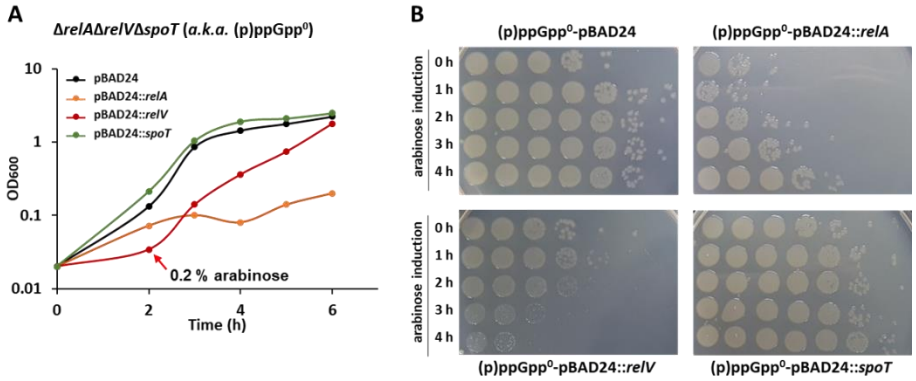

Figure 2.3. Effects of SR enzymes overexpression on (p)ppGpp^0 strain growth and viability. (A) Growth curves of (p)ppGpp^0 strains harboring the recombinant-pBAD24 plasmids. Bacterial cells were inoculated in LB-ampicillin broth and grown in aerobic condition. 0.2% arabinose was treated at OD_{600} ~ 0.1. (B) Viable cell plating of the indicated strains is shown in panel (A). Each bacterial strain was serially diluted and spotted on LB-ampicillin plates.

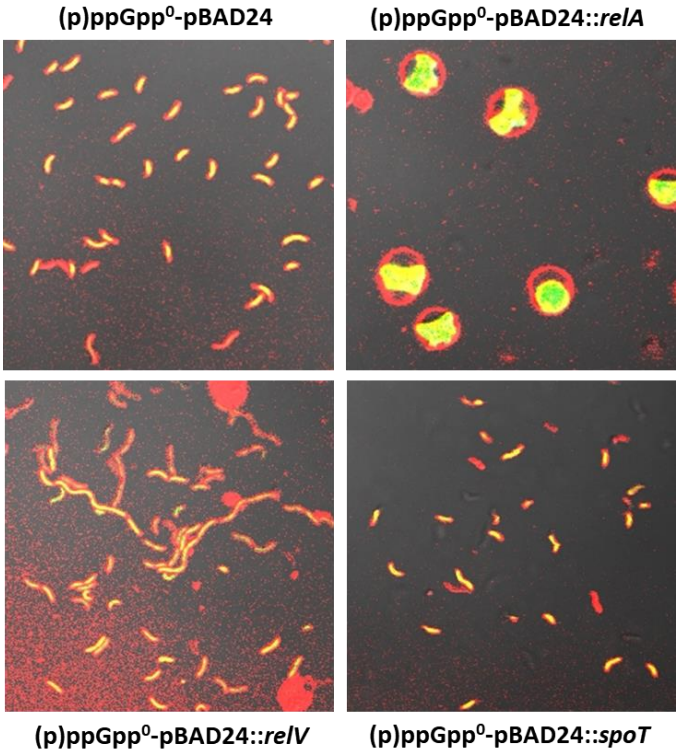

Figure 2.4. Confocal microscopic analysis of SR enzymes-overexpressed (p)ppGpp^0 strains. Confocal microscopic analysis of bacterial DNA and cell membrane. Arabinose induction followed the same condition as indicated in Figure 2.3 and bacterial cells were collected at 2 hr post arabinose induction. Each bacterial strain was stained with 0.05% Syto-9 (green fluorescence) and 0.05% FM4-64 (red fluorescence). Both green and red fluorescent images were merged with DIC images.

C. VC1223, located at the downstream of *relV* gene, showed partial anti-toxic effects on RelV-mediated toxicity

Our results showed that RelV, a SAS of *V. cholerae*, represented toxic effects on bacterial cells when overexpressed. The RelV-overproduction gradually increases bacterial death and elongation of intoxicated cells, as opposed to the RelA-induced effects. We previously discovered that *E. coli* strains slightly recovered their viabilities when VC1223 protein was co-expressed with *relV* gene (Fig. 2.2). Despite the fact that *VC1223* gene product does not share any structural similarity with the Tis1 antitoxin of *P. aeruginosa* PA14 strain, we hypothesized that VC1223 might also exert an antitoxic effect against the RelV-mediated toxicity. To address this hypothesis, we constructed Δ*relA*Δ*relV*Δ*VC1223*Δ*spoT* quadruple *V. cholerae* mutant in which all three SR genes and VC1223 coding genes are deleted. Like (p)ppGpp^0 mutant strains, we induced RelV and VC1223 proteins in this quadruple mutant via arabinose treatment. VC1223 protein did not affect bacterial growth or viability when it was expressed alone (Fig. 2.5A). Compared to *relV* sole expression, *relV-VC1223* co-expression did not significantly recover the lagged bacterial growth (Fig. 2.5A). In terms of CFU counting however, the strain that expressed both genes exhibited a better survival than that solely expressed *relV*. The number of viable cells at each time point was ~10-fold higher when the *VC1223* gene was co-expressed (Fig. 2.5B). From these results, we found that VC1223 could partially ameliorate the toxic effects of RelV. To further investigate the antitoxic

effects of VC1223, we conducted scanning electron microscopic (SEM) analysis to observe phenotypic changes in VC1223-expressing cells. The Δ*relA*Δ*relV*Δ*VC1223*Δ*spoT* mutant had almost identical cell morphology to (p)ppGpp^0 strains of Figure 2.4 when it harbored either a control plasmid or a RelA induction vector (Fig. 2.6). As expected, the quadruple mutants expressing RelV protein were elongated like a tree branch (Fig. 2.6). On the other hand, unfortunately, it was difficult to find neither phenotypic recovery nor shortening of bacterial cells in RelV-VC1223 co-expression group (Fig. 2.6). Taken together, although there was no dramatical restoration of RelV-inducible characteristics, VC1223 could partially neutralize the RelV toxicity by its unknown antitoxic mechanism.

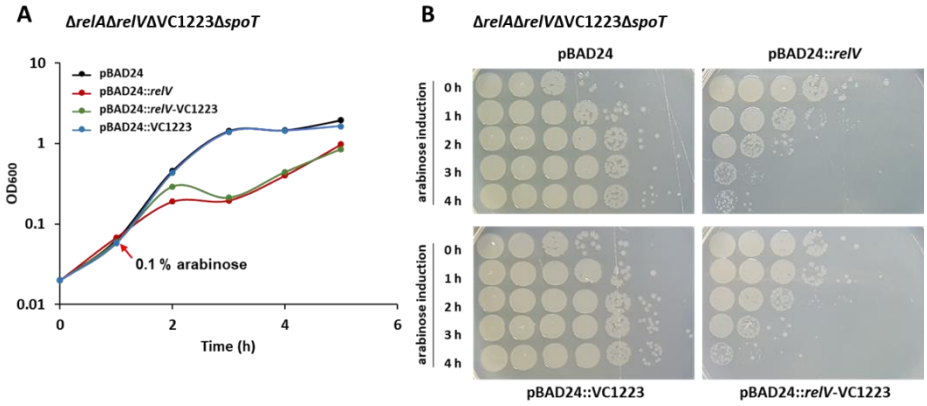

Figure 2.5. Effects of VC1223 co-expression on RelV toxicity in Δ*relA*Δ*relV* *VC1223*Δ*spoT* quadruple mutant. (A) Growth curves of Δ*relA*Δ*relV* Δ*VC1223*Δ*spoT* strains carrying the recombinant-pBAD24 plasmids. Bacterial cells were inoculated in LB-ampicillin broth and incubated anaerobically. 0.1% arabinose was treated at OD_{600} ~ 0.1. (B) Bacterial cell viabilities of the indicated strains are shown in panel (A). Each bacterial strain was serially diluted and spotted on LB-ampicillin containing plates.

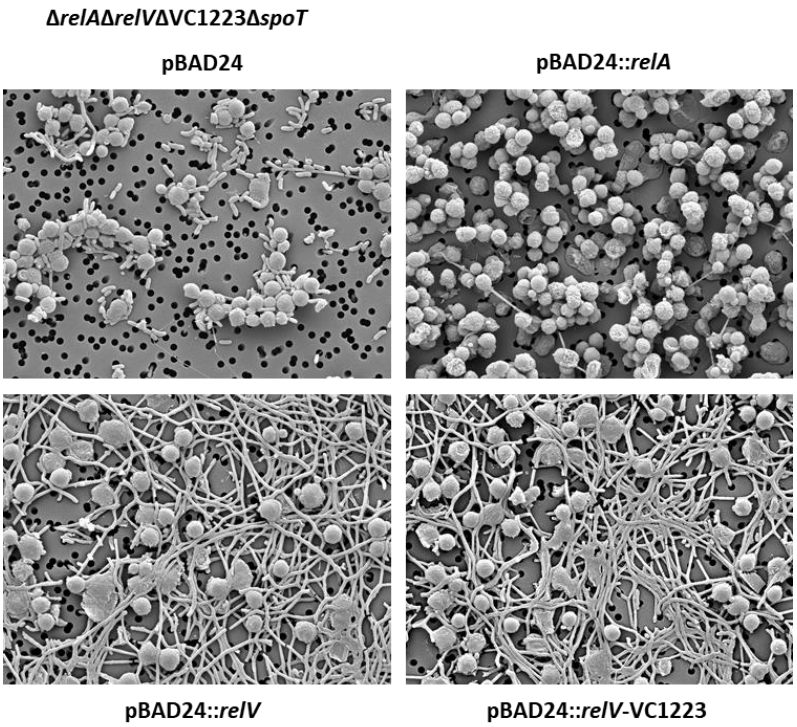

Figure 2.6. Scanning electron microscopic analysis of Δ*relA*Δ*relV*Δ*VC1223* Δ*spoT* strains harboring VC1223 expression vectors. Scanning electron microscopic analysis of Δ*relA*Δ*relV*Δ*VC1223*Δ*spoT* strains harboring the indicated plasmids. All bacterial strains were grown under identical conditions as described in Figure 2.5 and collected at 2hrs after arabinose induction.

D. RelA and RelV produce distinct sets of nucleotide derivatives

So far, our results demonstrated that (i) predicted structure of *V. cholerae* RelV protein resembles the structure of (p)ppApp producer, *P. aeruginosa* Tas1, (ii) the overexpression of *relV* leads to bacterial cell death as opposed to *relA* expression, (iii) co-expression of *VC1223* with *relV* genes partially restored RelV-mediated toxicity. These findings led us to postulate that the products of RelV enzyme are bactericidal, while the products of RelA are likely bacteriostatic. From our previous TLC analysis,[41] we observed that Δ*relA*Δ*spoT* mutant, known as a (p)ppGpp-accumulating mutant, produced the phosphate product spot which we determined as ppGpp.

Our conclusion was based on the findings that patterns of ^{32}P-labeled nucleotides were almost identical between the amino acid-starved wild type N16961 strain and its Δ*relA*Δ*spoT* mutant. However, as recent studies suggested that one-dimensional TLC analysis is insufficient in differentiating nucleotide derivatives that are similar in molecular weight,[122] two-dimensional TLC analysis was preferentially performed. To overexpress the three SR genes *relA*, *relV* and *spoT* in (p)ppGpp^0 mutant background, the strains were cultured in LB media containing ^{32}P. Indeed, our two-dimensional TLC successfully separated the overlapped spots undistinguishable in one-dimensional chromatography due to their similar molecular weight (Fig. 2.7A-D). We found that RelA and RelV enzymes produced several phosphate products which were not found in the (p)ppGpp^0 control group (Fig. 2.7A-C). The spot with white

arrows has been collectively determined as (p)ppGpp in one-dimensional TLC (Fig. 2.7B-D). The spot was substantially bigger in *relV*-expressed (p)ppGpp^0 mutant strain than the RelA-producing strain (Fig. 2.7B-C). An identical spot with very low quantity was also detected in SpoT-overproducing strain. These results indicate that RelV is probably the major enzyme for (p)ppGpp production and SpoT enzyme can also contribute to its production, albeit its level is marginal. (Fig. 2.7D). To our surprise, RelV-overproducing strain produced a couple of additional spots (blue and yellow) that are similar to the white spot in MW, (Fig. 2.7C). These new blue and yellow spots might not have been differentiated from the white spot in one-dimensional TLC. More importantly, the RelV-producing (p)ppGpp^0 strain also produced a dominant spot (green) that has a lower MW. Since this spot is not detected in other TLCs, it is highly likely that this green spot is one of the major products of RelV. (Fig. 2.7C). All in all, the *V. cholerae* strain, which expresses RelV protein, produces more varieties of phosphate products compared to RelA-producing cells. Two-dimensional TLC analysis showed previously undescribed nucleotide derivatives potentially involved in *V. cholerae* SR. To precisely identify those molecules and compare the production levels of each molecule among the samples, we will perform an additional analysis with Mass Spectrometry.

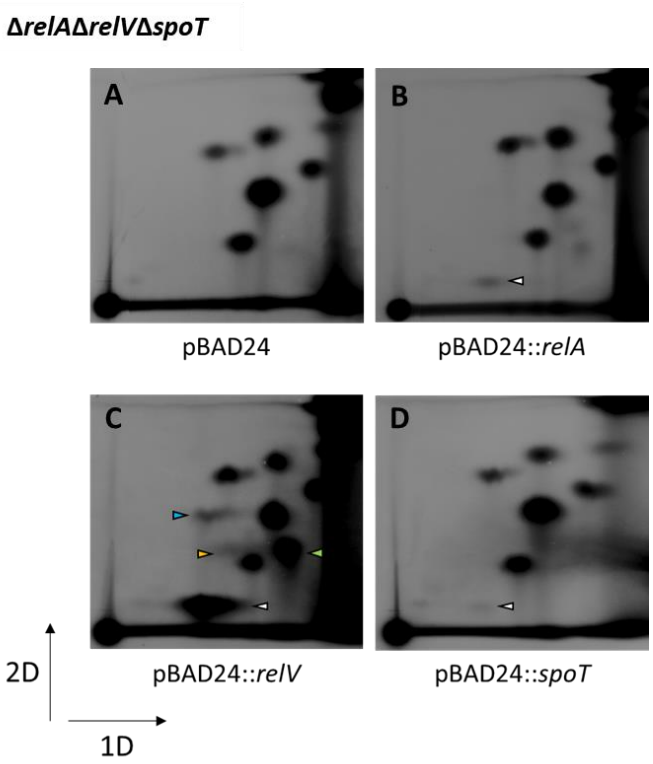

Figure 2.7. Two dimensional thin-layer chromatography analysis of *V. cholerae* strains harboring SR enzymes overexpression vectors. (A-D) All bacterial strains were grown under the identical conditions as Figure 2.3 in the presence of [^{32}P] orthophosphate and collected at 2hr post 0.2% arabinose treatment. Each lysate was spot inoculated on square TLC plates and developed with each 1 M LiCl and 4 M formic acid buffer and 0.85M KH_2PO_4 buffer (unadjusted pH) for first dimension and second dimension formation, respectively.

E. A transcriptomic analysis reveals that RelA and RelV regulate expression of distinct set of genes in *V. cholerae*

We discovered that two alarmone synthetase, RelA and RelV, produces different phosphate products which are not found in the (p)ppGpp^0 control group. We then sought to further elucidate the effects of products of RelA or RelV on genome-wide transcriptions. To this end, we conducted RNA sequencing with RelA- or RelV-producing (p)ppGpp^0 mutants, respectively. The (p)ppGpp^0 mutant harboring an empty plasmid was used as a normalization control. RNA samples were extracted from cells induced for 30 mins with arabinose in order to capture the immediate transcriptional changes. As a result, the overall transcriptomic landscape is clearly different between two inductions (Fig. 2.8B-C). All in all, a dramatic shift was more evident in RelV-overexpressing cells than RelA-producing groups. Transcription of 382 genes was strongly induced by *relV* overexpression, while a total of 90 genes were upregulated in their transcription in RelA-producing cells (Fig. 2.8A-C). The number of transcriptions downregulated by RelV and RelA were 55 and 75, respectively. Of particular interest, among 382 RelV-induced upregulations, only 40 genes are commonly upregulated by RelA as well (Fig. 2.8A-C). Likewise, only a small portion of the genes were commonly downregulated by RelA or RelV (Fig. 2.8A). These results strongly suggest that RelA- or RelV-mediated products likely regulate unique sets of genes. Because a larger number of genes were upregulated by RelV-mediated activity, we hypothesized that

RelV may act as a dominant regulator of *V. cholerae* SR (Fig. 2.8A,C). We then categorized meaningful transcriptional changes into distinct functional regulons (Fig. 2.8D-E). Remarkably, functional traits collectively categorized as *relA* regulons are rarely overlapped with *relV* regulons and these results once again suggested that RelA and RelV elicited completely distinct bacterial phenotypes. The pathway presenting the most significant increase by RelA expression was the siderophore metabolism involved in iron uptake (Fig. 2.8D). There was a substantial decrease in sugar uptake systems and flagellar synthesis (Fig. 2.8D). Moreover, the TCA cycle enzymes specifically involved in the synthetic pathway converting isocitrate to malate were also statistically reduced following RelA overexpression. By RelV, on the other hand, amino acid biosynthetic process pathways, especially branched amino acid biosynthesis pathways, were significantly upregulated (Fig. 2.8E). The increase in amino acid biosynthesis is a well-characterized outcome of SR induction.[7] In line with these findings, the amino acid transport system was downregulated when RelV was overproduced (Fig. 2.8E). We further discovered that the overall sulfate metabolisms were dramatically down-regulated following the RelV production (Fig. 2.8E). To sum up, these results clearly demonstrated that each RelA or RelV of *V. cholerae* induces substantially different regulons by producing their distinct products. Importantly, contrary to what was known, RelV regulates more globally than RelA on *V. cholerae* physiologies, such as amino acid

biosynthesis, the typical SR-inducing phenomenon.

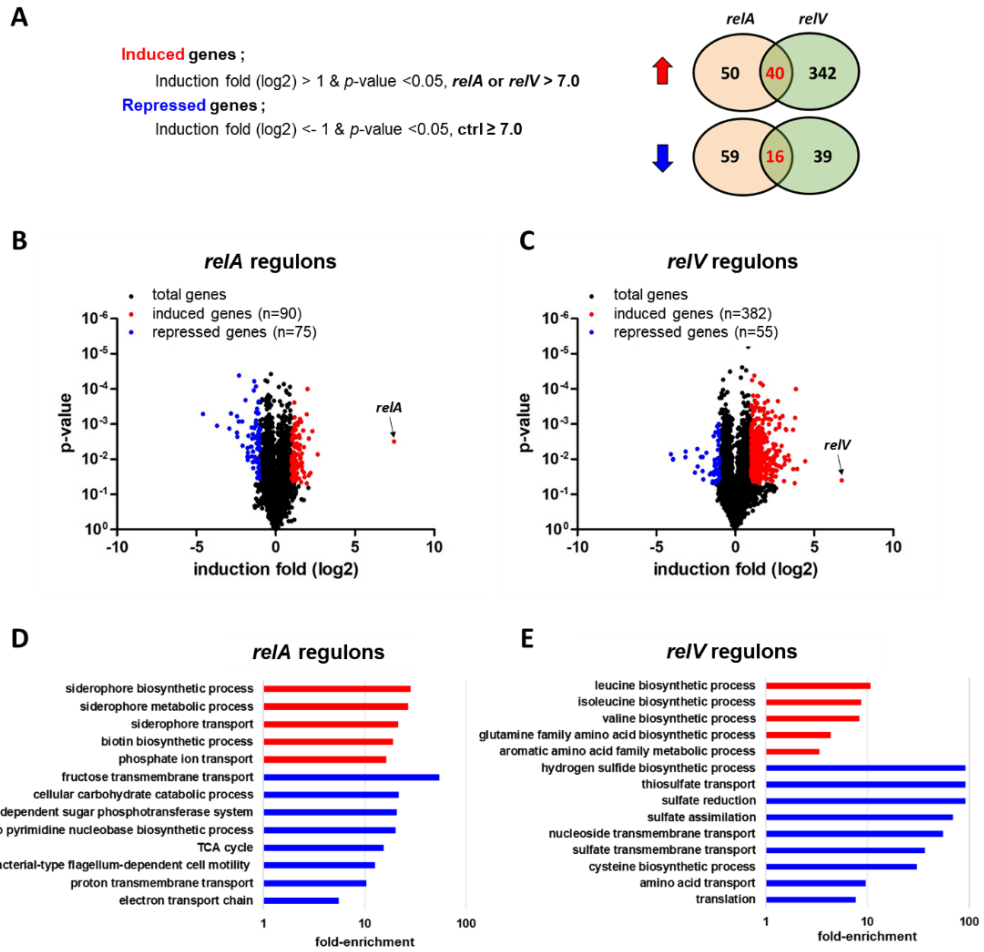

Figure 2.8. Transcriptomic analysis of (p)ppGpp^0 strains that depends on the each RelA or RelV enzyme expression. (A) The filtering conditions to sort out significant changes in each RelA or RelV expression compared to the control group. Venn diagrams show the number of genes that are up-regulated (red arrow) and down-regulated (blue arrow) in RelA- or RelV-dependent

manner. (B-C) Volcano plots of RelA- and RelV-regulons represented by indicated conditions in panel (A). The dots of induced genes are represented by red, and repressed genes are shown in blue. (D-E) Gene ontology (GO) analysis of each transcriptome which represents significant changes in RelA or RelV expression group. Individual gene categories show abundance of transcripts in each induced group (red bars) and repressed groups (blue bars).

F. RelV activity plays a more important role in regulating *V. cholerae* virulence

Our previous studies demonstrated that *V. cholerae* SR regulates its virulence and survival fitness in response to antibiotic treatment.[19,40,41] A long-standing question has been about which one of RelA or RelV plays a more crucial role in activating *V. cholerae* SR. Based on our results shown in Figure 2.7, RelV contributes to the production of diverse nucleotide derivatives, while RelA activity does it only at a minimal level. Importantly, our RNASeq analysis revealed that genes encoding several representative virulence determinants were expressed differently in response to RelA or RelV action (Fig. 2.9). Overall, virulence-associated genes were actively transcribed in cells containing active RelV. First, from our RNASeq results, we found that Vibrio polysaccharide synthesis (VPS) gene clusters (Cluster I – *vpsU*, *vpsA-K*, Cluster II – *vpsL-Q*), the major components of *V. cholerae* biofilm matrix, were substantially increased following *relV* expression (Fig. 2.9B). Moreover, VpsR and VpsT, the transcriptional activators of VPS clusters, were also induced in the RelV overexpression group by nearly two- or four-times more than the control and the RelA producing group, respectively (Fig. 2.9B). Consistent with these results, previous studies illustrated that the transcription of *vpsR* gene is strongly regulated by SR enzymes, especially RelV.[20] Additionally, the transcription of *cqsA*, which encodes CAI-1 autoinducer synthase, was also drastically increased in response to RelV action (Fig. 2.9B). These results

indicated that various components of biofilm maturation were significantly induced by RelV production. Based on these findings, we examined biofilm production of *V. cholerae* during the overexpression of RelA or RelV. Biofilms of *V. cholerae* N16961 strains were grown statically for 24 hrs and their maturation quantities were identified by confocal microscopic analysis. Consistent with our RNA seq data, the thickness of constructed biofilm was comparatively more robust in RelV-overexpressor than the control and RelA-overexpressed strains (Fig. 2.9C). This result suggested that RelV of *V. cholerae* highly induces the biofilm generation compared to RelA.

The initiation of biofilm formation in *V. cholerae* requires flagellum-mediated motility for the surface adherence.[127] We also discovered that several gene clusters involved in flagella assembly were differentially expressed in response to RelA vs. RelV production (Fig. 2.9D). The gene encoding flagellin monomers, *flaA-E*, was dramatically increased up to 5-fold following RelV production. In contrast, expression of *flaA-D* was was suppressed in RelA producing group (Fig. 2.9D). We then assessed the bacterial swimming motility on the soft agar plates supplemented with 0.1% arabinose. N16961 strains undergoing motility tests were containing either pBAD24, pBAD24::*relA* or pBAD24::*relV* vector. The tests were conducted by spot inoculation on the plates. Based on Figure 2.9E, *relV*-expressing cells are relatively more motile. Of note, swimming motility was substantially suppressed by *relA* gene expression. Next, we investigated the effects of RelA vs. RelV on cholera toxin

(CT) production. CT, a dominant virulence determinant, induces severe watery diarrhea in the host intestine. CT is encoded by *ctxA-B* operon in the genome of an integrated prophage CTXΦ. CTXΦ genome also possesses other virulence genes, encoding several accessory toxins near the *ctxAB* operon, such as zonula occludens toxin (Zot) and accessory cholera enterotoxin (Ace). Interestingly, we discovered that only *ctxAB* operon in CTXΦ prophage was significantly increased up to 4-fold under RelV production, while the transcription of other accessory toxin genes occurred at the similar level between the two groups (Fig. 2.9F). Moreover, during *relV* expression, *tcpA* to *tcpF* genes encoding the major colonization factor, toxin-coregulated pilus (TCP) of *V. cholerae*, were also invariably upregulated about 2-fold, while their expressions decreased approximately 2-fold in RelA- producing cells (Fig. 2.9F). To provide further evidence, we conducted a western blot analysis and compared the quantity of CT subunit B in bacterial supernatants. *V. cholerae* (p)ppGpp^0 strains producing each SR enzymes were grown *in vitro* with anaerobic TMAO respiration that stimulates CT production.[84] As a result, we found that CT production was markedly increased in cells with active RelV (Fig. 2.9G, red arrow). In contrast, CT production was not active in response to *relA* expression. (Fig. 2.9G). These results are consistent with our previous observation that Δ*relV* single deletion mutant, but not Δ*relA* mutant, showing a significant defect in CT production.[19] Together, these results clearly demonstrate that a range of virulence features in *V. cholerae* are positively

regulated by RelV-mediated activity while these phenotypes are rather inhibited by RelA action.

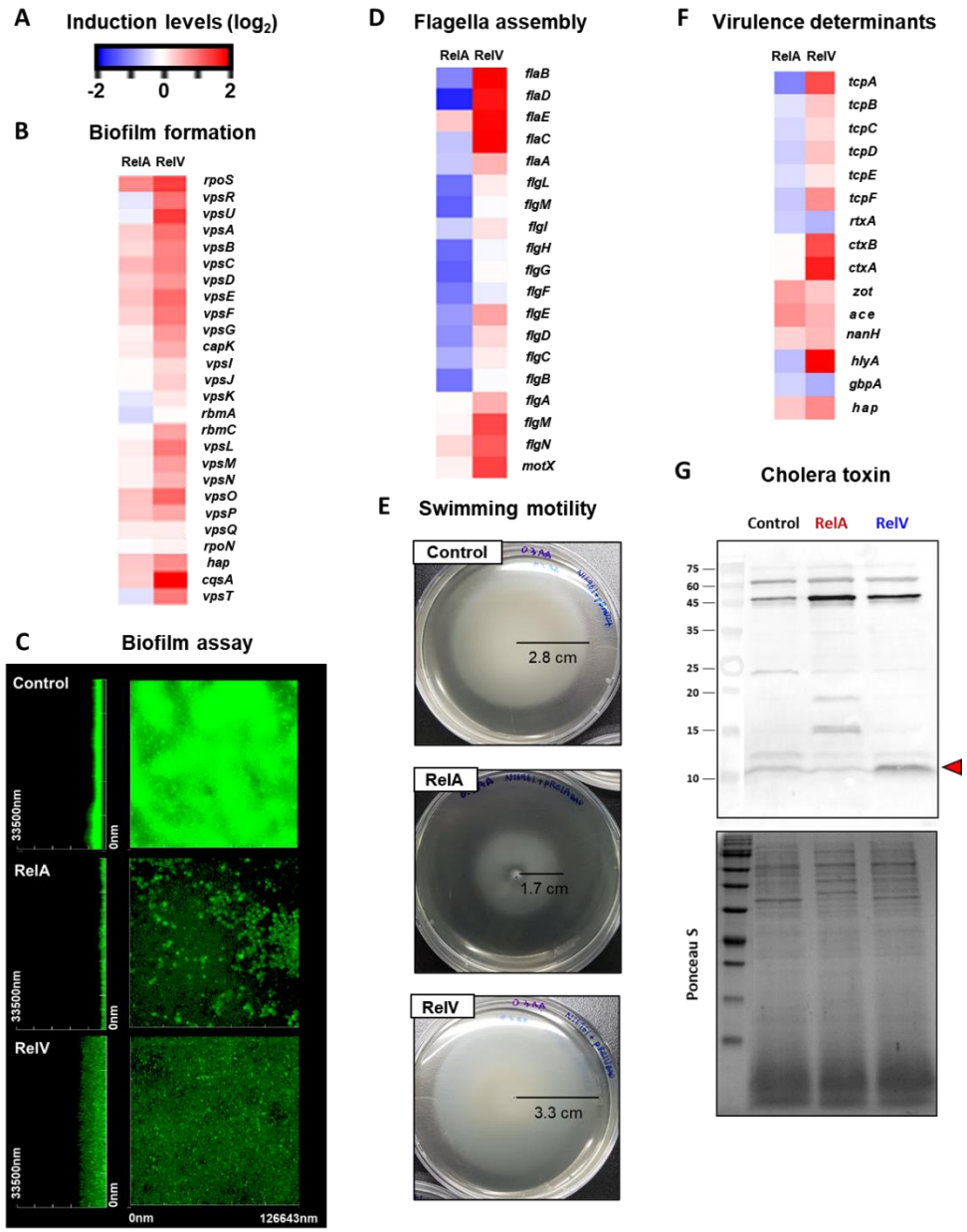

Figure 2.9. Comparative analysis of virulence factors dependent on RelA- and RelV-dependent manner. Each transcript induction level was quantified by log_2-normalized values of target genes (A) and represented as heat maps (B,D,F). (A) The induction levels ranging from -2.0 to 2.0 and shown in red and blue with relative upregulation and downregulation. (B) Transcripts level comparison of biofilm associated genes. (C) Confocal microscopic analysis to identify the biofilm formation. All bacterial strains were treated with 0.1% arabinose and statically incubated for 24 hrs. Planktonic bacteria of each culture was eliminated and residual biofilm was stained with 0.05% Syto9. (D) Transcript levels of genes encoding flagella assembly. (E) Swimming motility assay on 0.3% (w/v) agar LB plates. Bacterial strains were spot inoculated on the middle of plates and incubated 12 hrs at 30°C. (F) Transcriptional levels of genes encoding virulence determinants. (G) Western blot analysis of CT subunit B in (p)ppGpp^0 control and RelA-, RelV-producing groups. Bacterial strains were grown anaerobically, and each supernatant was extracted at 12 hr post arabinose induction and concentrated by TCA precipitation. 10 μg of all concentrated samples were loaded onto SDS-PAGE. The protein band that corresponds to the CT subunit B is shown with an arrowhead.

4. DISCUSSION

About 10 years have passed since a novel synthetase RelV was first discovered, but the specific function of RelV as a SR enzyme was poorly understood. Dasgupta and his colleagues showed that RelV synthesizes (p)ppGpp under glucose or fatty acid starvation in Δ*relA*Δ*spoT* mutant background.[65] The limitation of their study was that the analysis of TLC in single-dimension could not reveal the hidden products which drive distinctive characteristics. Though discovering that RelV is an additional (p)ppGpp producer to RelA, the studies could not find a significant difference between the regulon RelV and RelA. In our study, we proposed that RelV, a conserved SAS of *V. cholerae*, produces more virulent nucleotide products, compared to RelA. We examined the impact of *relV* and *relA* expressions under (p)ppGpp^0 background. As illustrated above, the limitation is that the condition set up for enzyme expression is very artificial, which is hard to happen spontaneously**.** Despite this limitation, we gained significant information that RelV is a major SR key-player which produces novel nucleotide alarmone that functions as a regulator and participates in more various metabolic pathways than another synthetase, RelA.

For several decades, RelA has been known as a major SR regulator in Gram-negative bacteria according to classical SR theory. The SR regulating function of RelA is triggered to synthesize (p)ppGpp when uncharged tRNA accumulates during amino acid starvation, leading to stalled ribosomes.

Consequently, activation of RelA in Gram-negative bacteria represses the capital regulons including stabilized RNA, ribosomal protein synthesis, cell wall synthesis and DNA replication. On the other hand, upon the activation of RpoS sigma factor-dependent regulons, universal stress proteins synthesis and amino acid biosynthesis are crucially increased against stress conditions. These are the canonical regulons which are elicited by SR. However, we discovered interesting results from *V. cholerae* RNA sequencing data. When *V. cholerae* (p)ppGpp^0 mutants solely expressed RelA or RelV protein, each transcriptomic tendency was clearly different in most pathways. Above all, in RelV expression, overall amino acids synthesis pathways were significantly increased, while amino acid transport was repressed (Fig. 2.8C). Moreover, ribosomal protein synthesis essential for translation was substantially decreased during RelV expression. Through these results, we clearly found that SR regulons like the metabolism and translation of amino acids are mostly regulated by RelV enzyme, and not by RelA in *V. cholerae*. In case of RelA, it also repressed the ribosomal protein synthesis, but it was not as significant as RelV regulation. Instead, RelA is more associated with iron uptake and central metabolism involved in energy production. From the previous study, we found that when *V. cholerae* undergoes SR, transcription of most TCA cycle enzymes is substantially decreased compared to control groups. It is clear that this phenomenon is derived by SR regulon, however, elucidation of the detailed mechanism is yet to be done. To sum up, based on these results, we expected

RelV to act as a first-line regulator for most metabolism associated with SR, and RelA to act as an additional regulator for metabolism which is not involved in RelV regulons. As our follow-up studies, we will investigate the biological roles of each regulon elicited by each enzyme under stress conditions.

From the previous study, Nielsen and his colleagues illustrated that RpoS of *V. cholerae* controls the mucosal escape which is evoked on the late infection stage.[44] They described that the genes encoding bacterial motility or chemotaxis was substantially increased by RpoS-dependent manner. These factors were essential for pathogens to escape from intestinal mucosa. In our RNA seq data, induction of *rpoS* gene expression is statistically valid under both RelA and RelV expressed condition, but the difference in the expression level between two enzymes was not significant. Moreover, chemotaxis gene expression was not notably changed in both RelA and RelV production. On the other hand, as shown in Figure 2.9D panel, *flaB-E* operon which encodes bacterial flagella filaments was significantly increased when RelV was expressed only. These results suggested that RelV and RpoS regulate bacterial motility and infection stage, respectively. We also discovered that biofilm producing genes significantly increased in accordance with RelV expression. Biofilm formation is crucial for the bacteria as it enhances the survival of pathogens in natural environments and facilitates the bacterial colonization when *V. cholerae* transmits to host intestinal tract.[128,129] In addition, robust expression of CT and TCP consequent to RelV production was detected, leading us to hypothesize

that RelV plays the essential role on initial infection stage, unlike RpoS regulation happening mostly in late infection stage. Therefore, based on these findings, further *in vivo* studies will be required to examine the virulence of RelV and trace the expression of each stringent response enzyme during host infection.

From our protein structure comparison, RelV showed a quite similar structure to Tas1 toxin domain. As we illustrated in Figure 2.1, RelV has an active domain highly homologous to the toxin domain of Tas1 protein (Fig. 2.1A). The findings that Tas1 and RelV share the identical active reaction sites that interact with ATP, the pyrophosphate donor was meaningful (Fig. 2.1B). Tas1, a T6SS effector protein of virulent *P. aeruginosa* strain PA14, drives drastic accumulation of (p)ppApp and depletion of ATP in competitor cells, eventually resulting in cell death.[120] The difference here is that *relV* gene encoded by *VC1224* is conserved by operon with *VC1223* on its downstream, while *tas1* gene is surrounded by T6SS cluster genes. Still, we could not find the potential T6SS cluster around *relV-VC1223* operon. In addition, other than *tas1* and its T6SS cluster, we found a potential signal peptide of *relV*, which might be regulated by Sec system, on its N-terminal domain (Fig. 2.1A). From our observations so far, we suggested the possibility that RelV might be transferred to periplasmic space by Sec system and delivered to other cells, unlike Tas1 secretion which is regulated by T6SS. Before then, we wondered whether RelV acts as a potential T6SS effector protein for interbacterial

interaction of *V. cholerae* and other species. First, we conducted a competition assay by co-culturing the *E. coli* BL21 strain with *V. cholerae* N16961 strains, which carry pBAD24 plasmid or overproduce RelV protein. As a result, regardless of experimental groups, we discovered that all N16961 strains were outcompeted by BL21 strains (data not shown). These results indicate that while *V. cholerae* is more advantageous than *E. coli* in survival under the contact-promoting conditions that facilitate T6SS attack, this phenomenon does not occur in RelV-dependent manner. Next, we sought for an alternative secretion mechanism in which RelV of *V. cholerae* uses to affect adjacent cells. The examination of whether RelV could be released to the extracellular space by its signal peptide consisting of 20 amino acids sequence on its N-terminal domain was carried out first. We recruited three kinds of protein pool - intracellular, periplasmic, and extracellular spaces- from RelV-overexpressing *V. cholerae*. As expected, RelV protein was detected respectively in the intracellular, and periplasmic fraction (data not shown). However, no RelV-band was detected in the extracellular protein pool. Although several clues led us to investigate whether RelV utilizes secretory mechanisms to affect neighboring cells, the results implied that RelV has no correlation with extracellular secretion so far.

Our results demonstrated that *relV-VC1223* genes, found in bicistronic loci, attain toxin-antitoxin systems against exposure to toxins. Though incomplete, VC1223 can diminish the RelV toxicity by its antitoxic activity and partially

recovers from the virulence. There was a study describing undiscovered SAS-based toxin (toxSAS) TA systems by using in silico sequencing search.[121] They also found that all of the toxSAS subfamilies with antitoxin are in a bicistronic or overlapping manner. We focused on evolutionary intimacy of *V. cholerae* RelV and FaRel (Firmicutes and Actinobacteria Rel) subfamily. FaRel-SAS is an enzyme found in multiple species of Firmicutes and Actinobacteria phylum. FaRel system is encoded in a conserved three-gene operon and that toxSAS gene is flanked by two neighboring antitoxin genes, each of which is sufficient to counteract the virulence. Out of the validated five subfamilies of toxSAS toxin which differ in the strength of the toxic effect, FaRel toxin is relatively weaker than other subfamilies. Interestingly, RelV in our research, resembles FaRel toxin in terms of a toxic strength and its synthetic products. However, the compositions of its neighboring antitoxin gene are different from that of FaRel subfamily. We found an upstream gene of RelV (*VC1225*) which has an opposite direction to *relV-VC1223* operon unlike FaRel subfamily. While FaRel toxicity is completely neutralized by its two antitoxins, VC1223 only partially alleviates the effects of RelV. This result can be illustrated by the antitoxic ability of the downstream FaRel antitoxin, which is less effective than the upstream antitoxin. We still wonder why *V. cholerae* possesses the genes derived from Firmicutes and Actinobacteria rather than Proteobacteria species, and why RelV exists as a two gene-operon rather than an intact three gene-operon like FaRel. It might be possible that RelV toxicity, which VC1223 was

unable to defend against, could be restored by hydrolase activity of SpoT. However, even in the absence of SpoT, the Δ*relA*Δ*spoT*,[41] Δ*relA*Δ*VC1223*-Δ*spoT* mutants of *V. cholerae* exhibits minimal growth albeit exposure to the nucleotide alarmones produced by RelV. To sum up, this indicates that an undiscovered complex network exists to regulate RelV expression even if it is not an extracellular stimulus.

In the previous study,[120] SpoT failed to alleviate Tas1 product ppApp, as it regenerated ADP. They found that the ppGpp hydrolase domain of SpoT was less active on ppApp than ppGpp *in vitro*. Although not shown in the main text, we overexpressed RelA and RelV enzymes in Δ*relA*Δ*relV* mutant strain of which SpoT remains in *V. cholerae*. Unlike (p)ppGpp^0 strain, Δ*relA*Δ*relV* mutant did not lose its viability even when RelA and RelV proteins were overproduced. However, when we overexpressed RelV in *E. coli* BL21 strain, SpoT of BL21 could not attenuate RelV toxicity and the strain rapidly lost its viabilities as a consequence. This dramatic fatality was fully recovered by the co-expression of *V. cholerae* SpoT. Together, we concluded from the result that the products of RelV can only be neutralized by SpoT of *V. cholerae*. Nevertheless, additional research is required to elucidate the mechanism of how *V. cholerae* SpoT alleviates the RelV toxicity, unlike *E. coli* SpoT. The difference might have derived from the distinction between both enzyme structures and other neutralizing products synthesized by *V. cholerae* SpoT. Though numerous trials were conducted to purify the RelV protein for *in vitro*

enzymatic assay, however, it was challenging to attain pure RelV protein. So, alternative analysis for quantifying the nucleotides products should be preceded to discover the relationship between RelV toxicity and SpoT activity in *V. cholerae*.

Through this study, we could describe the distinct roles of both *V. cholerae* alarmone synthetases, RelA and RelV, in stringent response (summarized in Fig. 2.10). First, we investigated the bacterial phenotypes when (p)ppGpp^0 mutant strains overexpressed each RelA or RelV protein. RelA overproduced-*V. cholerae* displayed a typical dormant cell shape of *Vibrio* species, while RelV expression killed the bacteria itself dramatically. We demonstrated that these different phenotypes are elicited by distinct products of each RelA or RelV enzyme. Furthermore, we discovered regulons of each enzyme, which responds to each alarmone synthetase expression. Remarkably, RelV induces more global pathways which have known as representative stringent response, such as the increase in amino acid biosynthesis and the substantial decrease in translation. In case of RelA, its expression leads to increased iron uptake and reduced carbohydrate catabolism plus nucleotide metabolism in contrast to RelV. Above all, we clearly demonstrated that RelV is an important upstream regulator of representative virulence factors in *V. cholerae*. All things considered, in *V. cholerae*, the novel SAS RelV and its products act as major regulators of bacterial physiology while RelA enzyme works as a major regulator in other bacteria species. Unfortunately, it is still unknown which key

factors cause the bacteria to undergo dormancy or cell death when *V. cholerae* expressed RelA or RelV enzyme, respectively. To understand the physiological roles of RelV and RelA during stress conditions, we will further conduct high-throughput mutational screening to discover the mutants which have defects on key pathways to elicit each enzyme phenotype.

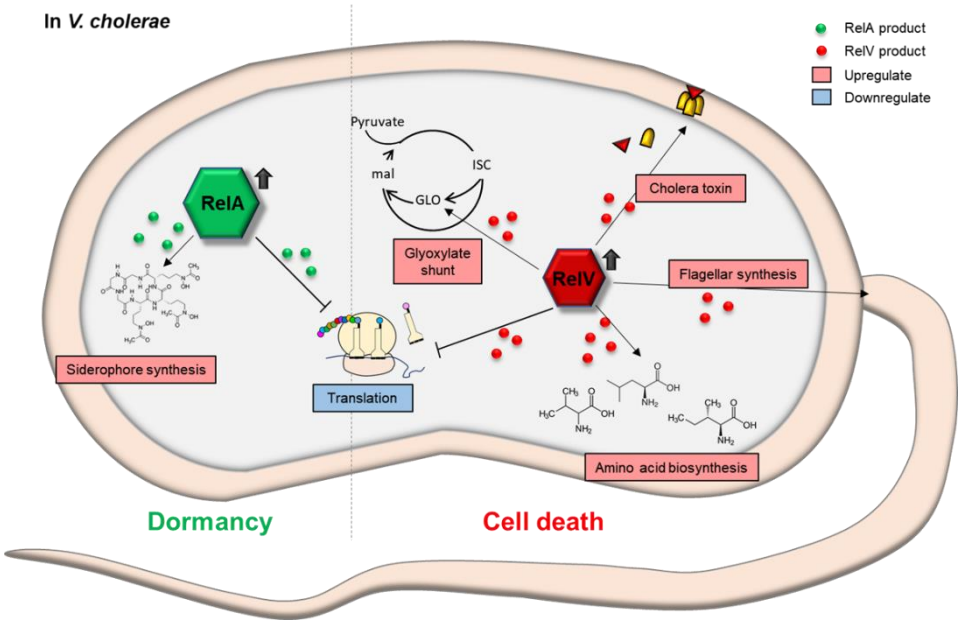

Figure 2.10. Summary of overall metabolic regulation elicited by both alarmone synthetase, RelA and RelV in *V. cholerae*. When bacteria face various stresses, SR enzymes are induced to regulate global metabolism using their distinctive regulons. In accordance with RelA expression, RelA specific products are synthesized, which highly up-regulate the siderophore synthesis associated with iron uptake. In case of RelV, its association with metabolism is more diversified, and the interaction is rarely overlapped with RelA regulons. Importantly, the regulons induced by RelV consist of major virulence factors of *V. cholerae*.

Chapter IV. CONCLUSION

In conclusion, this work reports that bacterial SR regulates antibiotic tolerance by diminishing the ROS production (Part II). Moreover, undescribed products and role of RelV, the unique SAS of *V. cholerae*, is revealed by molecular biologic basis studies (Part III). *V. cholerae* is a severe pathogen still needs to resolve in many developing countries. Our results suggest that SR regulates global metabolism of *V. cholerae* resulting in stress-tolerant states that arrest bacterial growth and express virulence factors. It should be noted that those phenotypes are differently regulated by each SR enzymes, RelA and RelV. In the meantime, we had been focusing on the relationship between SR and pathogenic properties of *V. cholerae* but, we found that there was a limitation to understand detail bacterial physiology at the enzyme level. We expect our current study to help elucidate the bona fide role of each SR enzymes in the *V. cholerae* pathogenic life cycle.

REFERENCES

1. Haseltine WA, Block R, Gilbert W, Weber K. MSI and MSII made on ribosome in idling step of protein synthesis. Nature 1972;238:381-4.
2. Cashel M, Kalbacher B. J. Biol. Chem. 1970;245.
3. Ross W, Vrentas Catherine E, Sanchez-Vazquez P, Gaal T, Gourse Richard L. The Magic Spot: A ppGpp Binding Site on E. coli RNA Polymerase Responsible for Regulation of Transcription Initiation. Molecular Cell 2013;50:420-9.
4. Zuo Y, Wang Y, Steitz Thomas A. The Mechanism of E. coli RNA Polymerase Regulation by ppGpp Is Suggested by the Structure of their Complex. Molecular Cell 2013;50:430-6.
5. Mechold U, Potrykus K, Murphy H, Murakami KS, Cashel M. Differential regulation by ppGpp versus pppGpp in Escherichia coli. Nucleic Acids Research 2013;41:6175-89.
6. Ronneau S, Hallez R. Make and break the alarmone: regulation of (p)ppGpp synthetase/hydrolase enzymes in bacteria. FEMS Microbiol Rev 2019;43:389-400.
7. Magnusson LU, Farewell A, Nyström T. ppGpp: a global regulator in Escherichia coli. Trends in Microbiology;13:236-42.
8. Hauryliuk V, Atkinson GC, Murakami KS, Tenson T, Gerdes K. Recent functional insights into the role of (p)ppGpp in bacterial physiology. Nat Rev Micro 2015;13:298-309.
9. Dalebroux ZD, Swanson MS. ppGpp: magic beyond RNA polymerase. Nat Rev Micro 2012;10:203-12.
10. Seyfzadeh M, Keener J, Nomura M. spoT-dependent accumulation of guanosine tetraphosphate in response to fatty acid starvation in Escherichia coli. Proc Natl Acad Sci U S A 1993;90:11004-8.
11. Battesti A, Bouveret E. Acyl carrier protein/SpoT interaction, the switch linking SpoT-dependent stress response to fatty acid metabolism.

Molecular Microbiology 2006;62:1048-63.

12. Haugen SP, Ross W, Gourse RL. Advances in bacterial promoter recognition and its control by factors that do not bind DNA. Nature Reviews Microbiology 2008;6:507-19.
13. Österberg S, del Peso-Santos T, Shingler V. Regulation of alternative sigma factor use. Annu Rev Microbiol 2011;65:37-55.
14. Jishage M, Kvint K, Shingler V, Nyström T. Regulation of sigma factor competition by the alarmone ppGpp. Genes & development 2002;16:1260-70.
15. Gaca AO, Colomer-Winter C, Lemos JA. Many means to a common end: the intricacies of (p)ppGpp metabolism and its control of bacterial homeostasis. Journal of Bacteriology 2015.
16. Kanjee U, Ogata K, Houry WA. Direct binding targets of the stringent response alarmone (p)ppGpp. Mol Microbiol 2012;85:1029-43.
17. Dalebroux ZD, Svensson SL, Gaynor EC, Swanson MS. ppGpp Conjures Bacterial Virulence. Microbiology and Molecular Biology Reviews 2010;74:171-99.
18. Nguyen D, Joshi-Datar A, Lepine F, Bauerle E, Olakanmi O, Beer K, et al. Active Starvation Responses Mediate Antibiotic Tolerance in Biofilms and Nutrient-Limited Bacteria. Science 2011;334:982-6.
19. Oh YT, Park Y, Yoon MY, Bari W, Go J, Min KB, et al. Cholera Toxin Production during Anaerobic Trimethylamine N-Oxide Respiration Is Mediated by Stringent Response in Vibrio cholerae. Journal of Biological Chemistry 2014;289:13232-42.
20. He H, Cooper JN, Mishra A, Raskin DM. Stringent Response Regulation of Biofilm Formation in Vibrio cholerae. Journal of Bacteriology 2012;194:2962-72.
21. Faruque SM, Albert MJ, Mekalanos JJ. Epidemiology, Genetics, and Ecology of ToxigenicVibrio cholerae. Microbiology and Molecular

Biology Reviews 1998;62:1301-14.

22. Kaper JB, Morris JG, Levine MM. Cholera. Clinical Microbiology Reviews 1995;8:48-86.
23. Sikora AE. Proteins Secreted via the Type II Secretion System: Smart Strategies of Vibrio cholerae to Maintain Fitness in Different Ecological Niches. PLoS Pathogens 2013;9:e1003126.
24. Leibovici-Weissman Y, Neuberger A, Bitterman R, Sinclair D, Salam MA, Paul M. Antimicrobial drugs for treating cholera. Cochrane Database Syst Rev 2014:CD008625.
25. Sack DA, Sack RB, Nair GB, Siddique AK. Cholera. The Lancet 2004;363:223-33.
26. Kaper JB, Moseley SL, Falkow S. Molecular characterization of environmental and nontoxigenic strains of Vibrio cholerae. Infection and Immunity 1981;32:661.
27. Bhattacharya MK, Bhattacharya SK, Garg S, Saha PK, Dutta D, Nair GB, et al. Outbreak of Vibrio cholerae non-O1 in India and Bangladesh. Lancet 1993;341:1346-7.
28. Jonson G, Holmgren J, Svennerholm AM. Analysis of expression of toxin-coregulated pili in classical and El Tor Vibrio cholerae O1 in vitro and in vivo. Infection and immunity 1992;60:4278-84.
29. Gill DM, Rappaport RS. Origin of the enzymatically active A1 fragment of cholera toxin. J Infect Dis 1979;139:674-80.
30. Cassel D, Selinger Z. Mechanism of adenylate cyclase activation by cholera toxin: inhibition of GTP hydrolysis at the regulatory site. Proc Natl Acad Sci U S A 1977;74:3307-11.
31. Miller VL, Taylor RK, Mekalanos JJ. Cholera toxin transcriptional activator toxR is a transmembrane DNA binding protein. Cell 1987;48:271-9.
32. Sigel SP, Payne SM. Effect of iron limitation on growth, siderophore

production, and expression of outer membrane proteins of Vibrio cholerae. Journal of bacteriology 1982;150:148-55.

33. Higgins DE, DiRita VJ. Genetic analysis of the interaction between Vibrio cholerae transcription activator ToxR and toxT promoter DNA. Journal of bacteriology 1996;178:1080-7.

34. Yoon SS, Mekalanos JJ. 2,3-butanediol synthesis and the emergence of the Vibrio cholerae El Tor biotype. Infect Immun 2006;74:6547-56.

35. Jubair M, Morris JG, Ali A. Survival of Vibrio cholerae in Nutrient-Poor Environments Is Associated with a Novel “Persister” Phenotype. PLoS ONE 2012;7:e45187.

36. Brenzinger S, van der Aart LT, van Wezel GP, Lacroix J-M, Glatter T, Briegel A. Structural and Proteomic Changes in Viable but Non-culturable Vibrio cholerae. Frontiers in microbiology 2019;10:793-.

37. Teschler JK, Zamorano-Sánchez D, Utada AS, Warner CJA, Wong GCL, Linington RG, et al. Living in the matrix: assembly and control of Vibrio cholerae biofilms. Nature reviews. Microbiology 2015;13:255-68.

38. Geiger T, Francois P, Liebeke M, Fraunholz M, Goerke C, Krismer B, et al. The stringent response of Staphylococcus aureus and its impact on survival after phagocytosis through the induction of intracellular PSMs expression. PLoS Pathog 2012;8:e1003016.

39. Kim HY, Yu SM, Jeong SC, Yoon SS, Oh YT. Effects of flaC Mutation on Stringent Response-Mediated Bacterial Growth, Toxin Production, and Motility in Vibrio cholerae. J Microbiol Biotechnol 2018;28:816-20.

40. Oh YT, Lee K-M, Bari W, Raskin DM, Yoon SS. (p)ppGpp, a Small Nucleotide Regulator, Directs the Metabolic Fate of Glucose in Vibrio cholerae. Journal of Biological Chemistry 2015;290:13178-90.

41. Kim HY, Go J, Lee KM, Oh YT, Yoon SS. Guanosine tetra- and

pentaphosphate increase antibiotic tolerance by reducing reactive oxygen species production in Vibrio cholerae. J Biol Chem 2018;293:5679-94.

42. Dasgupta S, Basu P, Pal RR, Bag S, Bhadra RK. Genetic and mutational characterization of the small alarmone synthetase gene relV of Vibrio cholerae. Microbiology 2014;160:1855-66.
43. Haralalka S, Nandi S, Bhadra RK. Mutation in the relA Gene of Vibrio cholerae Affects In Vitro and In Vivo Expression of Virulence Factors. Journal of Bacteriology 2003;185:4672-82.
44. Nielsen AT, Dolganov NA, Otto G, Miller MC, Wu CY, Schoolnik GK. RpoS controls the Vibrio cholerae mucosal escape response. PLoS Pathog 2006;2:e109.
45. Oh YT, Kim HY, Kim EJ, Go J, Hwang W, Kim HR, et al. Selective and Efficient Elimination of Vibrio cholerae with a Chemical Modulator that Targets Glucose Metabolism. Frontiers in Cellular and Infection Microbiology 2016;6:156.
46. Matson JS, Withey JH, DiRita VJ. Regulatory networks controlling Vibrio cholerae virulence gene expression. Infect Immun 2007;75:5542-9.
47. Thelin KH, Taylor RK. Toxin-coregulated pilus, but not mannose-sensitive hemagglutinin, is required for colonization by Vibrio cholerae O1 El Tor biotype and O139 strains. Infection and Immunity 1996;64:2853-6.
48. Childers BM, Klose KE. Regulation of virulence in Vibrio cholerae: the ToxR regulon. Future Microbiology 2007;2:335-44.
49. Krebs SJ, Taylor RK. Protection and attachment of Vibrio cholerae mediated by the toxin-coregulated pilus in the infant mouse model. J Bacteriol 2011;193:5260-70.
50. Patra FC, Sack DA, Islam A, Alam AN, Mazumder RN. Oral

rehydration formula containing alanine and glucose for treatment of diarrhoea: a controlled trial. BMJ : British Medical Journal 1989;298:1353-6.

51. Greenough WB, III, Rosenberg IS, Gordon RS, Jr., Davies BI, Benenson AS. TETRACYCLINE IN THE TREATMENT OF CHOLERA. The Lancet;283:355-7.
52. Lindenbaum J, Greenough WB, Islam MR. Antibiotic therapy of cholera. Bulletin of the World Health Organization 1967;36:871-83.
53. Rahaman MM, Majid MA, Alam AKMJ, Islam MR. Effects of Doxycycline in Actively Purging Cholera Patients: a Double-Blind Clinical Trial. Antimicrobial Agents and Chemotherapy 1976;10:610-2.
54. Roy SK, Islam A, Ali R, Islam KE, Khan RA, Ara SH, et al. A randomized clinical trial to compare the efficacy of erythromycin, ampicillin and tetracycline for the treatment of cholera in children. Transactions of The Royal Society of Tropical Medicine and Hygiene 1998;92:460-2.
55. Kaushik JS, Gupta P, Faridi MMA, Das S. Single dose azithromycin versus ciprofloxacin for cholera in children: A randomized controlled trial. Indian Pediatrics 2009;47:309-15.
56. De S, Chaudhuri A, Dutta P, Dutta D, De SP, Pal SC. Doxycycline in the treatment of cholera. Bulletin of the World Health Organization 1976;54:177-9.
57. Weber JT, Mintz ED, Cañizares R, Semiglia A, Gomez I, Sempértegui R, et al. Epidemic cholera in Ecuador: multidrug-resistance and transmission by water and seafood. Epidemiology and Infection 1994;112:1-11.
58. Towner KJ, Pearson NJ, Mhalu FS, O'Grady F. Resistance to antimicrobial agents of Vibrio cholerae El Tor strains isolated during

the fourth cholera epidemic in the United Republic of Tanzania. Bulletin of the World Health Organization 1980;58:747-51.

59. Wang R, Lou J, Liu J, Zhang L, Li J, Kan B. Antibiotic resistance of Vibrio cholerae O1 El Tor strains from the seventh pandemic in China, 1961–2010. International Journal of Antimicrobial Agents 2012;40:361-4.

60. Jesudason M. Change in serotype and appearance of tetracycline resistance in V. cholerae O1 in Vellore, South India. Indian Journal of Medical Microbiology 2006;24:152-3.

61. Chomvarin C, Johura F-T, Mannan SB, Jumroenjit W, Kanoktippornchai B, Tangkanakul W, et al. Drug response and genetic properties of Vibrio cholerae associated with endemic cholera in north-eastern Thailand, 2003–2011. Journal of Medical Microbiology 2013;62:599-609.

62. Mandal J, Dinoop KP, Parija SC. Increasing Antimicrobial Resistance of Vibrio cholerae OI Biotype EI Tor Strains Isolated in a Tertiary-care Centre in India. Journal of Health, Population, and Nutrition 2012;30:12-6.

63. Klontz EH, Das SK, Ahmed D, Ahmed S, Chisti MJ, Malek MA, et al. Long-term comparison of antibiotic resistance in Vibrio cholerae O1 and Shigella species between urban and rural Bangladesh. Clin Infect Dis 2014;58:e133-6.

64. Potrykus K, Cashel M. (p)ppGpp: Still Magical? Annual Review of Microbiology 2008;62:35-51.

65. Das B, Pal RR, Bag S, Bhadra RK. Stringent response in Vibrio cholerae: genetic analysis of spoT gene function and identification of a novel (p)ppGpp synthetase gene. Molecular Microbiology 2009;72:380-98.

66. Aedo S, Tomasz A. Role of the Stringent Stress Response in the

Antibiotic Resistance Phenotype of Methicillin-Resistant Staphylococcus aureus. Antimicrobial Agents and Chemotherapy 2016;60:2311-7.

67. Kim C, Mwangi M, Chung M, Milheirço C, de Lencastre H, Tomasz A. The Mechanism of Heterogeneous Beta-Lactam Resistance in MRSA: Key Role of the Stringent Stress Response. PLOS ONE 2013;8:e82814.
68. Abranches J, Martinez AR, Kajfasz JK, Chávez V, Garsin DA, Lemos JA. The Molecular Alarmone (p)ppGpp Mediates Stress Responses, Vancomycin Tolerance, and Virulence in Enterococcus faecalis. Journal of Bacteriology 2009;191:2248-56.
69. Wu J, Long Q, Xie J. (p)ppGpp and drug resistance. Journal of Cellular Physiology 2010;224:300-4.
70. Ishiguro EE, Ramey WD. Inhibition of in vitro peptidoglycan biosynthesis in Escherichia coli by guanosine 5′-diphosphate 3′-diphosphate. Canadian Journal of Microbiology 1980;26:1514-8.
71. Rodionov DG, Ishiguro EE. Direct correlation between overproduction of guanosine 3',5'-bispyrophosphate (ppGpp) and penicillin tolerance in Escherichia coli. Journal of Bacteriology 1995;177:4224-9.
72. Heath RJ, Jackowski S, Rock CO. Guanosine tetraphosphate inhibition of fatty acid and phospholipid synthesis in Escherichia coli is relieved by overexpression of glycerol-3-phosphate acyltransferase (plsB). Journal of Biological Chemistry 1994;269:26584-90.
73. Greenway DLA, England RR. The intrinsic resistance of Escherichia coli to various antimicrobial agents requires ppGpp and σs. Letters in Applied Microbiology 1999;29:323-6.
74. Hesketh A, Hill C, Mokhtar J, Novotna G, Tran N, Bibb M, et al. Genome-wide dynamics of a bacterial response to antibiotics that target the cell envelope. BMC Genomics 2011;12:226.
75. Khakimova M, Ahlgren HG, Harrison JJ, English AM, Nguyen D. The

Stringent Response Controls Catalases in Pseudomonas aeruginosa and Is Required for Hydrogen Peroxide and Antibiotic Tolerance. Journal of Bacteriology 2013;195:2011-20.

76. Kohanski MA, Dwyer DJ, Hayete B, Lawrence CA, Collins JJ. A Common Mechanism of Cellular Death Induced by Bactericidal Antibiotics. Cell;130:797-810.
77. Lobritz MA, Belenky P, Porter CBM, Gutierrez A, Yang JH, Schwarz EG, et al. Antibiotic efficacy is linked to bacterial cellular respiration. Proceedings of the National Academy of Sciences 2015;112:8173-80.
78. Dwyer DJ, Belenky PA, Yang JH, MacDonald IC, Martell JD, Takahashi N, et al. Antibiotics induce redox-related physiological alterations as part of their lethality. Proceedings of the National Academy of Sciences 2014;111:E2100-E9.
79. Yoon MY, Min KB, Lee K-M, Yoon Y, Kim Y, Oh YT, et al. A single gene of a commensal microbe affects host susceptibility to enteric infection. Nature Communications 2016;7:11606.
80. Philippe N, Alcaraz J-P, Coursange E, Geiselmann J, Schneider D. Improvement of pCVD442, a suicide plasmid for gene allele exchange in bacteria. Plasmid 2004;51:246-55.
81. Yoon MY, Lee K-M, Park Y, Yoon SS, Kaushal D. Contribution of Cell Elongation to the Biofilm Formation of Pseudomonas aeruginosa during Anaerobic Respiration. PLoS One 2011;6:e16105.
82. Fonseca NA, Marioni J, Brazma A. RNA-Seq Gene Profiling - A Systematic Empirical Comparison. PLoS ONE 2014;9:e107026.
83. Possel H, Noack H, Augustin W, Keilhoff G, Wolf G. 2,7-Dihydrodichlorofluorescein diacetate as a fluorescent marker for peroxynitrite formation. FEBS Letters 1997;416:175-8.
84. Lee K-M, Park Y, Bari W, Yoon MY, Go J, Kim SC, et al. Activation of Cholera Toxin Production by Anaerobic Respiration of Trimethylamine

N-oxide in Vibrio cholerae. The Journal of Biological Chemistry 2012;287:39742-52.

85. Jang S, Imlay JA. Hydrogen peroxide inactivates the Escherichia coli Isc iron-sulfur assembly system, and OxyR induces the Suf system to compensate. Molecular microbiology 2010;78:1448-67.

86. Pal RR, Bag S, Dasgupta S, Das B, Bhadra RK. Functional characterization of the stringent response regulatory gene dksA of Vibrio cholerae and its role in modulation of virulence phenotypes. J Bacteriol 2012;194:5638-48.

87. Dalebroux ZD, Svensson SL, Gaynor EC, Swanson MS. ppGpp conjures bacterial virulence. Microbiol Mol Biol Rev 2010;74:171-99.

88. Ronayne EA, Wan YCS, Boudreau BA, Landick R, Cox MM. P1 Ref Endonuclease: A Molecular Mechanism for Phage-Enhanced Antibiotic Lethality. PLOS Genetics 2016;12:e1005797.

89. Wang X, Kim Y, Ma Q, Hong SH, Pokusaeva K, Sturino JM, et al. Cryptic prophages help bacteria cope with adverse environments. Nature Communications 2010;1:147.

90. Imlay JA, Chin SM, Linn S. Toxic DNA damage by hydrogen peroxide through the Fenton reaction in vivo and in vitro. Science 1988;240:640.

91. Jang S, Imlay JA. Micromolar Intracellular Hydrogen Peroxide Disrupts Metabolism by Damaging Iron-Sulfur Enzymes. Journal of Biological Chemistry 2007;282:929-37.

92. Brandt KG, Castro Antunes MM, Silva GA. Acute diarrhea: evidence-based management. J Pediatr (Rio J) 2015;91:S36-43.

93. Das JK, Ali A, Salam RA, Bhutta ZA. Antibiotics for the treatment of Cholera, Shigella and Cryptosporidium in children. BMC Public Health 2013;13 Suppl 3:S10.

94. Mwansa JCL, Mwaba J, Lukwesa C, Bhuiyan NA, Ansaruzzaman M, Ramamurthy T, et al. Multiply antibiotic-resistant Vibrio cholerae O1

biotype El Tor strains emerge during cholera outbreaks in Zambia. Epidemiology and Infection 2007;135:847-53.

95. Sugisaki K, Hanawa T, Yonezawa H, Osaki T, Fukutomi T, Kawakami H, et al. Role of (p)ppGpp in biofilm formation and expression of filamentous structures in Bordetella pertussis. Microbiology 2013;159:1379-89.

96. Jiang M, Sullivan SM, Wout PK, Maddock JR. G-Protein Control of the Ribosome-Associated Stress Response Protein SpoT. Journal of Bacteriology 2007;189:6140-7.

97. Yoon MY, Lee K, Yoon SS. Protective role of gut commensal microbes against intestinal infections. Journal of Microbiology 2014;52:983-9.

98. Potrykus K, Murphy H, Philippe N, Cashel M. ppGpp is the major source of growth rate control in E. coli. Environmental microbiology 2011;13:563-75.

99. Gaca AO, Kajfasz JK, Miller JH, Liu K, Wang JD, Abranches J, et al. Basal Levels of (p)ppGpp in Enterococcus faecalis: the Magic beyond the Stringent Response. mBio 2013;4.

100. Maisonneuve E, Castro-Camargo M, Gerdes K. (p)ppGpp Controls Bacterial Persistence by Stochastic Induction of Toxin-Antitoxin Activity. Cell 2013;154:1140-50.

101. Maisonneuve E, Gerdes K. Molecular Mechanisms Underlying Bacterial Persisters. Cell 2014;157:539-48.

102. Lewis K. Persister Cells. Annual Review of Microbiology 2010;64:357-72.

103. Wyckoff EE, Mey AR, Leimbach A, Fisher CF, Payne SM. Characterization of Ferric and Ferrous Iron Transport Systems in Vibrio cholerae. Journal of Bacteriology 2006;188:6515-23.

104. Griffiths GL, Sigel SP, Payne SM, Neilands JB. Vibriobactin, a siderophore from Vibrio cholerae. Journal of Biological Chemistry

1984;259:383-5.

105. Mey AR, Wyckoff EE, Oglesby AG, Rab E, Taylor RK, Payne SM. Identification of the Vibrio cholerae Enterobactin Receptors VctA and IrgA: IrgA Is Not Required for Virulence. Infection and Immunity 2002;70:3419-26.

106. Wyckoff EE, Valle A-M, Smith SL, Payne SM. A Multifunctional ATP-Binding Cassette Transporter System from Vibrio cholerae Transports Vibriobactin and Enterobactin. Journal of Bacteriology 1999;181:7588-96.

107. Rogers MB, Sexton JA, DeCastro GJ, Calderwood SB. Identification of an Operon Required for Ferrichrome Iron Utilization in Vibrio cholerae. Journal of Bacteriology 2000;182:2350-3.

108. Davies BW, Bogard RW, Mekalanos JJ. Mapping the regulon of Vibrio cholerae ferric uptake regulator expands its known network of gene regulation. Proceedings of the National Academy of Sciences 2011;108:12467-72.

109. Brynildsen MP, Liao JC. An integrated network approach identifies the isobutanol response network of <em>Escherichia coli</em&gt. Molecular Systems Biology 2009;5.

110. Baharoglu Z, Mazel D. Vibrio cholerae Triggers SOS and Mutagenesis in Response to a Wide Range of Antibiotics: a Route towards Multiresistance. Antimicrobial Agents and Chemotherapy 2011;55:2438-41.

111. Wexselblatt E, Oppenheimer-Shaanan Y, Kaspy I, London N, Schueler-Furman O, Yavin E, et al. Relacin, a Novel Antibacterial Agent Targeting the Stringent Response. PLOS Pathogens 2012;8:e1002925.

112. Ronneau S, Caballero-Montes J, Coppine J, Mayard A, Garcia-Pino A, Hallez R. Regulation of (p)ppGpp hydrolysis by a conserved archetypal regulatory domain. Nucleic Acids Res 2019;47:843-54.

113. Cao M, Kobel PA, Morshedi MM, Wu MF, Paddon C, Helmann JD. Defining the Bacillus subtilis sigma(W) regulon: a comparative analysis of promoter consensus search, run-off transcription/macroarray analysis (ROMA), and transcriptional profiling approaches. J Mol Biol 2002;316:443-57.

114. D'Elia MA, Millar KE, Bhavsar AP, Tomljenovic AM, Hutter B, Schaab C, et al. Probing teichoic acid genetics with bioactive molecules reveals new interactions among diverse processes in bacterial cell wall biogenesis. Chem Biol 2009;16:548-56.

115. Geiger T, Kästle B, Gratani FL, Goerke C, Wolz C. Two small (p)ppGpp synthases in Staphylococcus aureus mediate tolerance against cell envelope stress conditions. J Bacteriol 2014;196:894-902.

116. Weinrick B, Dunman PM, McAleese F, Murphy E, Projan SJ, Fang Y, et al. Effect of mild acid on gene expression in Staphylococcus aureus. J Bacteriol 2004;186:8407-23.

117. Steinchen W, Schuhmacher JS, Altegoer F, Fage CD, Srinivasan V, Linne U, et al. Catalytic mechanism and allosteric regulation of an oligomeric (p)ppGpp synthetase by an alarmone. Proc Natl Acad Sci U S A 2015;112:13348-53.

118. Xiao H, Kalman M, Ikehara K, Zemel S, Glaser G, Cashel M. Residual guanosine 3',5'-bispyrophosphate synthetic activity of relA null mutants can be eliminated by spoT null mutations. J Biol Chem 1991;266:5980-90.

119. Dedrick RM, Jacobs-Sera D, Bustamante CAG, Garlena RA, Mavrich TN, Pope WH, et al. Prophage-mediated defence against viral attack and viral counter-defence. Nature Microbiology 2017;2:16251.

120. Ahmad S, Wang B, Walker MD, Tran H-KR, Stogios PJ, Savchenko A, et al. An interbacterial toxin inhibits target cell growth by synthesizing (p)ppApp. Nature 2019;575:674-8.

121. Jimmy S, Saha CK, Kurata T, Stavropoulos C, Oliveira SRA, Koh A, et al. A widespread toxin−antitoxin system exploiting growth control via alarmone signaling. Proceedings of the National Academy of Sciences 2020;117:10500-10.
122. Sobala M, Bruhn-Olszewska B, Cashel M, Potrykus K. Methylobacterium extorquens RSH Enzyme Synthesizes (p)ppGpp and pppApp in vitro and in vivo, and Leads to Discovery of pppApp Synthesis in Escherichia coli. Front Microbiol 2019;10:859.
123. Lee K, Lee KM, Kim D, Yoon SS. Molecular Determinants of the Thickened Matrix in a Dual-Species Pseudomonas aeruginosa and Enterococcus faecalis Biofilm. Appl Environ Microbiol 2017;83.
124. Min KB, Yoon SS. Transcriptome analysis reveals that the RNA polymerase-binding protein DksA1 has pleiotropic functions in Pseudomonas aeruginosa. J Biol Chem 2020;295:3851-64.
125. Traxler MF, Summers SM, Nguyen H-T, Zacharia VM, Hightower GA, Smith JT, et al. The global, ppGpp-mediated stringent response to amino acid starvation in Escherichia coli. Molecular Microbiology 2008;68:1128-48.
126. Kim H-M, Yoon C-K, Ham H-I, Seok Y-J, Park Y-H. Stimulation of Vibrio vulnificus Pyruvate Kinase in the Presence of Glucose to Cope With H(2)O(2) Stress Generated by Its Competitors. Frontiers in microbiology 2018;9:1112-.
127. Giacomucci S, Cros CD-N, Perron X, Mathieu-Denoncourt A, Duperthuy M. Flagella-dependent inhibition of biofilm formation by sub-inhibitory concentration of polymyxin B in Vibrio cholerae. PloS one 2019;14:e0221431-e.
128. Seper A, Pressler K, Kariisa A, Haid AG, Roier S, Leitner DR, et al. Identification of genes induced in Vibrio cholerae in a dynamic biofilm system. International journal of medical microbiology : IJMM

2014;304:749-63.

129. Fong JCN, Syed KA, Klose KE, Yildiz FH. Role of Vibrio polysaccharide (vps) genes in VPS production, biofilm formation and Vibrio cholerae pathogenesis. Microbiology (Reading) 2010;156:2757-69.

ABSTRACT(IN KOREAN)

콜레라 원인균 *Vibrio cholerae*의 생존에 세균의 스트레스 반응기전인 Stringent response가 미치는 작용기제

< 지도교수 윤상선 >

연세대학교 대학원 의과학과

김화영

급성 설사병 콜레라를 일으키는 원인 균주인 *Vibrio cholerae*는 여전히 많은 개발도상국에서 해결되지 않는 문제로 남아있다. *V. cholerae*가 만들어내는 독성 인자에는 cholera toxin (CT), toxin-co-regulated pilus (TCP)가 있는데, 이 인자들은 *V. cholerae* 균이 숙주의 장내에서 다량의 물이 설사로 빠져나가게 하는 역할을 맡고 있다. 최근 다양한 선행연구들을 통해, 특이적인 뉴클레오타이드 생산물인 (p)ppGpp로 인해 발생되는 세균의 스트레스 반응기전인 stringent response (SR)가 이러한 *V. cholerae*의 독성 인자들과 생존을 조절할 수 있다고 확인되었

다. 우리는 이번 연구에서 SR이 *V. cholerae*의 항생제 저항성을 높이는 데 기여하는 작용 기전을 밝혔고 (Chapter II), 나아가 *V. cholerae*에 특이적으로 존재하는 SR 효소인 RelV가 (p)ppGpp 뿐만이 아니라 새로운 뉴클레오타이드 생산물을 생산할 수 있는 가능성을 확인했다 (Chapter III).

Chapter II에서 우리는 *V. cholerae* N16961 균주에서 (p)ppGpp를 합성하거나 분해하는 세 가지 효소, *relA*, *relV* 그리고 *spoT* 유전자를 모두 없앤 돌연변이 균주 (p)ppGpp^{0}가 야생형 N16961 균주에 비해 현저히 항생제에 대한 저항성이 낮은 것을 확인하였다. 이에, (p)ppGpp0 돌연변이주에 transposon (Tn) 스크리닝 방법으로 (p)ppGpp^0 균주 바탕임에도 항생제에 저항성을 보이는 돌연변이주를 찾아냈고, 그 균주에 *acnB* 유전자에 Tn이 삽입된 것을 확인했다. *acnB*는 TCA 회로에 관여하는 aconitase B를 코딩하는 유전자이며, 이 유전자를 비롯해 TCA 회로에 관여하는 여러 효소의 유전자들을 없앤 돌연변이 균주들은 모두 항생제에 저항성을 가지게 되었다. 이를 통해 *V. cholerae*의 항생제 저항성에 호기성 대사작용인 TCA회로가 상당히 중요한 역할을 한다고 판단할 수 있었는데, 우리는 호기 조건이 아닌 혐기 조건, 즉 TCA 회로가 작용하지 못하는 조건에서는 항생제에 대한 저항성이 SR에 의존적이지 않고 모두 증가한다는 것을 알아냈다. 또한 철이온 킬레이트제를 처리한 조건에서도 항생제에 대한 저항

성이 모두 증가하였고, 이는 항생제 저항성에 활성산소 (ROS)의 생산이 결정적인 역할을 한다는 것을 알 수 있었다. 무엇보다도, (p)ppGpp^0 돌연변이주는 3가 철이온을 세포 내로 운반하는 FbpA 단백질이 증가하며, 이 때문에 활성산소 생산에 사용되는 철이온이 야생형 N16961에 비해 세포 내에 많이 존재하게 되어 항생제에 대한 저항성이 떨어지는 것을 확인할 수 있었다. 우리는 이 연구를 통해 SR이 세포 내의 중심대사와 활성산소를 유발하는 철 이온의 습득을 억제함으로써 *V. cholerae*가 항생제에 내성을 가지게 한다는 것을 입증하였다.

Chapter III에서는 *V. cholerae*의 세 가지 SR 효소 중 하나인 RelV에 대하여 집중적으로 연구하였다. RelV는 RelA, SpoT와는 다르게 오직 (p)ppGpp를 합성하는 domain만 가지고 있는 합성 효소이며, 세 가지 효소 중 가장 최근에 발견되어 아직 그 작용 기전에 대한 연구가 많지 않다. 최근에 녹농균 PA14 균주에서 세균의 공격 기전인 type 6 secretion system (T6SS)의 effector protein, Tas1이 (p)ppApp라는 독성 뉴클레오타이드 생산물을 만든다고 보고되었는데, 흥미롭게도 *V. cholerae*의 RelV의 구조가 Tas1와 매우 유사하다는 것을 알게 되었다. 이를 통해 RelV가 그 동안 우리가 알고 있던 (p)ppGpp 합성이 아닌 (p)ppApp를 생산하는 새로운 기능을 가질 수도 있다는 가설을 세웠고, 놀랍게도 RelA와 RelV를 *V. cholerae* 세포 내에서 과발현 시

켰을 때, RelA와 반대로 RelV는 세포의 사멸을 유도한다는 것을 확인하였다. 이러한 RelV의 독성은 *relV* 유전자의 바로 뒤에 존재하는 VC1223에 의해 일부 회복이 가능하였고, 이는 독소-항독소 작용기전과 유사해 보였다. 우리는 2차원 thin layer chromatography 실험을 통해 (p)ppGpp^0 돌연변이주에 RelV를 발현시킨 경우에는 RelA를 발현시켰을 때에는 존재하지 않는 다른 인산염 생산물이 만들어진다는 것을 확인하였고, LC/MS 기법으로 그 생산물을 동정하였다. 또한 RNA sequencing을 통해 RelA와 RelV를 발현시킨 *V. cholerae* 균주가 전혀 다른 regulon을 가진다는 것을 알아내어, 똑같이 SR에 관여하는 것으로 생각해왔던 두 효소가 각기 맡은 역할이 상당히 다르다는 것을 밝혀냈다.

종합하여, 이와 같은 연구 결과들은 SR이 *V. cholerae*의 생존과 독성에 상당한 조절 작용을 맡고 있다는 것을 입증하며, 한편으로 그러한 SR을 조금 더 세부적으로 연구하여 구체적인 각 효소들의 역할에 대해서도 연구하는 것이 중요하다는 것을 알려준다.

핵심되는 말 : *Vibrio cholerae*, Stringent response, 항생제 저항성, (p)ppGpp,

PUBLICATION LIST

Kim HY, Go J, Lee KM, Oh YT, Yoon SS. Guanosine tetra- and pentaphosphate increase antibiotic tolerance by reducing reactive oxygen species production in Vibrio cholerae. *J Biol Chem.* 2018;293:5679-94.

Kim HY, Yu SM, Jeong SC, Yoon SS, Oh YT. Effects of flaC Mutation on Stringent Response-Mediated Bacterial Growth, Toxin Production, and Motility in Vibrio cholerae. *J Microbiol Biotechnol.* 2018;28:816-20.